Norwegian University of Life Sciences

Master's Thesis 2022 60 ECTS

Faculty of Chemistry, Biotechnology and Food Science

Isomeric Separation of Branched PFOS Isomers: An application of C18 based stationary phases for liquid chromatographic separation

Mathias André Myhre Berntzen

Chemistry

Acknowledgements

With the hope of this thesis not being affected by the Covid-19 pandemic, most of this thesis was written in periods of restrictions which resulted in challenging circumstances. With delays in deliveries that ended up with multiple iterations of the aim of this thesis. This thesis has been made possible with the help and guidance from so many great people and they deserve my deepest gratitude.

I would like to thank you individually.

Supervisor Professor Roland Kallenborn, for providing an interesting and relevant subject and providing information to further understand the world of Analytical chemistry.

Postdoctoral researcher Ivo Havranek for introducing me to the lab practice at the start of the thesis and providing good research materials.

Senior engineer Erik Mangnus Ræder, for providing invaluable help with the practical lab work and dedicating his time to give input when direly needed. Your help will never be forgotten.

The period of this thesis through periodically stressful times have been made easier with support from my family and friends. Some of the key people deserve to be acknowledged.

I would like to show my gratitude for the people in my dorm “Trekrona” for providing a positive environment with laughter, good talks and activities.

I would also show appreciation for my mother and father or guiding me throughout my life so I could end up choosing a degree in chemistry.

I would like to show my deepest gratitude for Marthe Ahlgreen Hansen for being my mental support through difficult and stressful times. This period would have been a lot more difficult without you, and for that I will always have a place for you in my heart.

This study was funded by the Research council of Norway (RCN) 268258 - Reducing the impact of fluorinated compounds on the environment and human health "

Abstract

Perfluorooctanesulfonate (PFOS) is a synthetic chemical that persist ubiquitously in waters and soils all over the world. PFOS has since its invention in the 1950 been one of the most produced per- and polyfluorinated alkylated substances (PFAS). The physical and chemical properties of PFOS is the reason it has been utilized in industrial sectors and household items as surfactants. The large area of applicability has consequently given multiple contamination sources. As a result of PFOS persistency in nature and links to multiple negative health effects, PFOS is classified as a persistent organic pollutant. A process called electrochemical fluorination (ECF) is the most common way to synthesize PFOS. This process synthesizes approximately 70% linear PFOS (L-PFOS) in addition to approximately 30% branched isomers of PFOS (Br-PFOS).

The objective of this study was to develop and validate an analytical method for quantification and separation of L-PFOS and 7 Br-PFOS isomers found in the technical product of PFOS by ECF. The analytical method was developed on a high-performance liquid chromatography tandem mass spectrometry (HPLC-MS/MS) instrument with an ACE Excel C18- PentaFluoroPhenyl (PFP) column. The method will attempt to quantitate the PFOS isomers individually in freshwater samples from a river in Fjellhamar, a lake called Sogna in Kjeller and run-off water from Ny-Ålesund to create an isomer profile for each location. The sample locations have possibilities of PFOS contamination from Aqueous Film-Forming Foam which is a major contamination source.

The method was validated and managed to separate the target isomers into 5 groups of PFOS, whereas 3 of them were single separated isomers, while the remaining 2 peaks consisted of coeluted isomers. Each group was treated as analytes and was applied to quantitate PFOS isomers in the water samples.

Both L-PFOS and Br-PFOS were detected at all sites proving that each study site had PFOS contamination. Some of the analytes were not at a detectable or quantifiable level in the samples from Fjellhamar river and Sogna, which showed that the method has sensitivity issues at low concentrations. All isomers were quantified in Ny-Ålesund, but some exceeded the linear range of the analytical method. The isomer profiles from all study sites found the contribution of L-PFOS to be below 60%, which provided insight in Br-PFOS different physical and chemical properties compared to L-PFOS.

Sammendrag

Perfluoroktylsulfonat (PFOS) er et syntetisk kjemikalie som finnes i vann og jord over hele verden. PFOS har siden sin oppfinnelse i 1950 vært en av de mest produserte per- og polyfluoralkyl stoffene. På grunn av sine fysiske og kjemiske egenskaper, er PFOS brukt særlig i industriell sektor og i husholdningsartikler som overflateaktivt middel. Det store bruksområdet har medført flere kilder til forurensing. Grunnet PFOS sin lange holdbarhet i naturen og kobling til flere negative helseeffekter, har PFOS blitt klassifisert som en persistent organisk miljøgift. En prosess kalt elektrokjemisk fluorering (ECF) er den vanligste måten å syntetisere PFOS på. Denne prosessen syntetiserer omtrent 70% lineær PFOS (L-PFOS), i tillegg til omtrent 30% forgrenede isomerer av PFOS (Br-PFOS).

Målet ved denne studien var å utvikle og validere en analytisk metode for kvantifisering og separering av L-PFOS og 7 Br-PFOS isomerer funnet i det tekniske produktet av PFOS ved hjelp av ECF. Den analytiske metoden ble utviklet for et høy-presisjons væskekromatografi tandem massespektrometer (HPLC-MS/MS), et instrument med en ACE Excel C18-pentafluorfenyl (PFP) kolonne. Denne metoden vil forsøke å kvantifisere PFOS isomerene individuelt i ferskvannsprøver fra en elv i Fjellhamar, innsjøen Sogna på Kjeller og avløpsvann fra Ny-Ålesund, hvor målet er å lage en isomer profil for hvert sted. Prøvetakingslokalitetene kan muligens være kontaminert av PFOS holdig brannskum (AFFF), som er en stor forurensningskilde til PFOS.

Metoden ble validert og klarte å separere målisomerene i fem grupper av PFOS, hvor tre av dem var enkelt separerte isomerer, mens de gjenstående to toppene besto av koeluerte isomerer. Hver gruppe ble behandlet som enkelte analytter og ble brukt for å kvantifisere PFOS isomerer i vannprøvene.

Både L-PFOS og Br-PFOS ble detektert på alle lokalitetene. Dermed ble det vist at hvert prøveområde hadde PFOS forurensing. I vannprøvene fra Fjellhamarelven og Sogna hadde noen av analyttene ikke målbare eller kvantifiserbare nivåer av PFOS, noe som viste at metoden har sensitivitetsproblemer ved lave konsentrasjoner. Alle isomerene ble kvantifisert i prøven fra Ny-Ålesund, men noen overskred den lineære rekkevidden av den analytiske metoden. Fra isomerprofilene fra alle prøveområdene ble det funnet at bidraget fra L-PFOS var under 60%, noe som ga innsikt i Br-PFOS ulike fysiske og kjemiske egenskaper sammenlignet med L-PFOS.

Contents_Toc108775609

Acronyms and abbreviations

AFFFs	Aqueous film-forming foams
ALT	Alanine transferase
BMI	Body mass index
Br-PFOS	Branched PFOS
CE	Collision energy
COP	Conference of parties
DDT	Dichlorodiphenyltrichloroethane
ECF	Electrochemical fluorination
FTS	Fluorotelomer sulfonate
GC	Gas chromatography
HETP	Height Equivalent to a Theoretical Plate
HF	Hydrofluoric acid
HPLC	High-performance liquid chromatography
HPLC-MSMS	High-performance liquid chromatography tandem mass spectroscopy
ISTD	Intern standard
IUPAC	The International Union of Pure and Applied Chemistry
LC	Liquid chromatography
L-PFOS	Linear PFOS
LOD	Limit of detection
LOQ	Limit of quantification
MeOH	Methanol
MPFOS	C13 marked Sodium perfluoro-1-[1,2,3,4-$^{13}C_4$] octanesulfonate
MRM	Multiple reaction monitoring
MS/MS	Mass analyzer
NH_4Ac	Ammonium acetate
OECD	The United Nations Organization of Economic Corporation and Development
PCB	Polychlorinated biphenyls
PFAAs	Perfluoroalkyl Acids
PFAS	Poly- and perfluoroalkyl substances
PFBS	Perfluorobutane sulfonate
PFOS	Perfluoro octane sulfonic acid
PFP	ACE excel C18-PentaFluoroPhenyl
PFSA	Perfluoroalkyl sulfonic acid
POP	Persistent organic pollutant
PTFE	Polytetrafluorethylene
QqQ	Triple quadrupole
SPE	Solid-phase extraction
T-PFOS	Technical PFOS
UHPLC	Ultra-high-precision liquid chromatography
WAX	Weak Anion Exchange

1. Introduction

General information and history

Poly- and perfluoroalkyl substances (PFAS) are a group of synthetic organic chemicals that persist ubiquitously in waters, soil and the atmosphere all over the world. The first perfluorinated compound was invented in the 1930s with the name polytetrafluorethylene (PTFE) and were used as a surfactant for non-stick products and impregnation of clothes due to its repellent characteristics. In 1940s and 1950s there were a prefoliation of new PFAS compounds being made. By replacing the hydrogens in organic chemicals with fluorine, creating a carbon fluorine bond, scientist created one of the strongest compounds in organic chemistry due to the electronegative properties of fluorine (Brennan et al., 2021; ITRC, 2020). Since the invention of the first PFAS chemicals, it is estimated that there are 5000 to 10000 chemicals in the PFAS family (USEPA, 2018). A report from 2018 identified around 4700 PFAS chemicals on the international market (OECD, 2018).

Perfluoro octane sulfonic acid (PFOS) was invented in the 1950s and is the most produced PFAS compound in the world (Abunada et al., 2020). This chemical have previously been present in aqueous film-forming foams (AFFFs), which was vastly used between 1970 and 1990 to extinguish hydrocarbon-based fuel fires at airports, oil refineries and municipal firefighting training sites (Houtz et al., 2013). PFOS is also used in the textile industry as surfactants (Sunderland et al., 2019).What makes PFAS stand out among other chemicals is the physical and chemical properties, which gives a wide area of use. The reason behind PFASs unique properties is their fluorinated carbon skeleton which will be further elaborated in this paper.

Definition and Structure

PFOS is defined as a persistent organic pollutant (POP) and has similar environmental properties with Dichlorodiphenyltrichloroethane commonly known as DDT and Polychlorinated biphenyls (PCB) (Buck et al., 2011). What makes PFAS stand out is its amphiphilic properties. Unlike other lipophilic POPs, the amphiphilic properties make PFAS chemicals susceptible to interact with both polar and non-polar solutions. A definition presented in a milestone paper by Buck et al (2011) defined PFAS as a chemical with one or more carbon atom where all hydrogen (H) substituents from its analogue have been partially or fully replaced with fluorine (F) atoms. From this definition, PFAS will have the molecular

formula C_nF_{2n+1}, which means it must have the presence of at least one $-CF_3$. A newer definition has been presented by OECD in 2021 with the intention of including fully fluorinated chemicals without a $-CF_3$ e.g., circular PFAS chemicals and chemicals with functional groups at all ends in a molecule.

All PFAS chemicals shares the same basic structure, although they can have different lengths and branching on the alkyl chain, differing degree of fluorination and functional groups which gives unique attributes. This makes it possible to categorize PFAS compounds into separate groups. The first categorization of PFAS is the classes; polymers and non-polymers. PFAS molecules that has been put together through repeating units or monomers, classifies as a polymer. Non-polymer PFAS can be divided into two subclasses: perfluoroalkyl- and polyfluoroalkyl substances. The degree of fluorination on the carbon skeleton, constitutes if a compound is a poly- or perfluoroalkyl substance. “Poly” is used if the compound is partially fluorinated and “per” is used if it is fully fluorinated.

PFOS is categorized as a non-polymer perfluoroalkyl substance and fall under the group Perfluoroalkyl Acids (PFAAs). PFOS is then put in the subgroup Perfluoroalkyl sulfonic acid (PFSA). Within the subgroup there are compounds that shares a similar structure to PFOS such as branched isomers of PFOS. The target analytes in this paper are branched isomers of PFOS, which in their entirety falls under the abbreviation branched PFOS (Br-PFOS) while linear PFOS gets the abbreviation L-PFOS. These branched isomers include per fluorinated monomethylated sulphonic acids and dimethylated sulphonic acids. The structure of PFAAs can be divided into two parts which consists of an acidic functional group usually called the head and the per- or polyfluorinated carbon chain called the tail (Buck et al., 2011).

Isomerism is a term used for chemical compounds with approximately the same molecular formula, but with varying chemical properties. Structure isomerism can be classified based on how the structural formula differs from each other. Molecules that have the same molecular formula but differs in the arrangement of the atoms is called structure isomeric. In regards of PFOS, there is 89 possible geometric isomers but only 11 are present in technical PFOS (T-PFOS) by ECF. There are currently only 7 isomers available on the market. The PFOS isomers relevant to this study is listed in table 1-1 and are all structure isomeric. This is because they all share the same molecular formula $C_8F_{17}SO_3$ and have different structures in the form of per fluorinated methyl groups. This means that the isomers relevant to this study shares the same molecular mass of 499 m/z.

PFAA can be broken into two subgroups, long chained and short chained based on the length of the alkyl chain. Long chained PFAAs contains at least an alkyl chain of 7 carbons or more. This means that L-PFOS is long chained as well as the monomethylated heptyl (C_7) branched isomers in this paper. Short chained PFAAs have a molecular structure with an alkyl chain with less than 7 carbons. The dimethylated branched isomers in this paper falls under this subgroup because of its hexyl (C_6) carbon chain (Buck et al., 2011).

Table 1-1: Name, abbreviations, and structure of PFOS and the isomers in this thesis

Isomer	Acronym	Structure
Perfluorooctane Sulfonate	L-PFOS	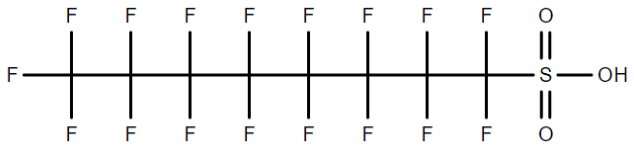
Perfluoro-1-methylheptane sulfonate	P1MHpS	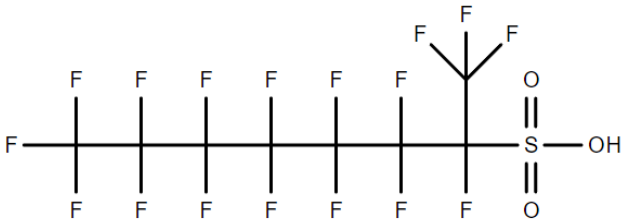
Perfluoro-3-methylheptane sulfonate	P3MHpS	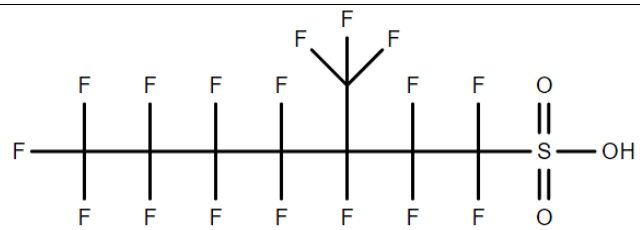
Perfluoro-4-methylheptane sulfonate	P4MHpS	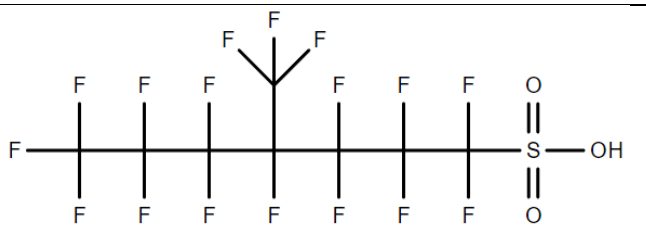
Perfluoro-5-methylheptane sulfonate	P5MHpS	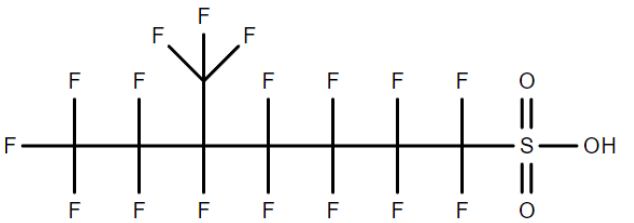

Table 1-1: Name, abbreviations, and structure of PFOS and the isomers in this thesis		
Perfluoro-6-methylheptane sulfonate	P6MHpS	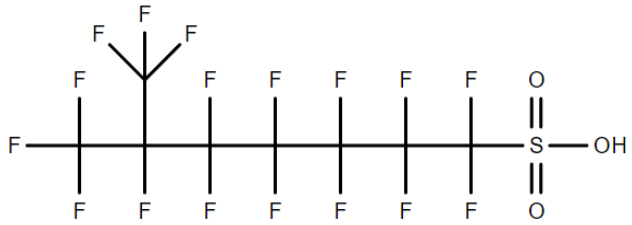
Perfluoro-4,5-dimethylhexane sulfonate	P45DMHxS	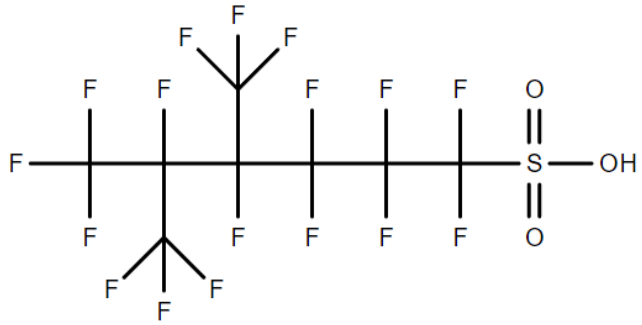
Perfluoro-3,5-dimethylhexane sulfonate	P35DMHxS	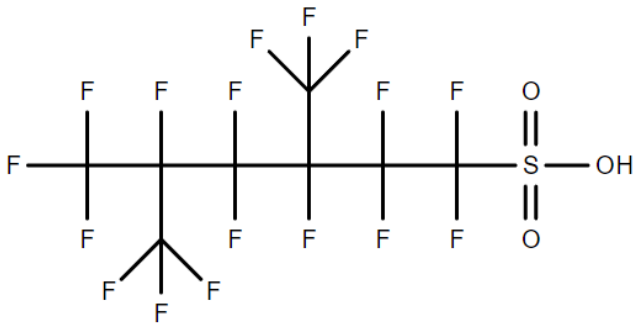
Perfluoro-5,5-dimethylhexane sulfonate	P55DMHxS	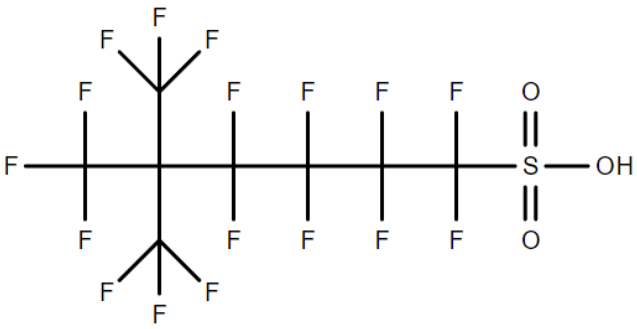

Terminology

The terminology for the scientific naming of PFAS in general varies from source to source. Both L-PFOS and Br-PFOS follows the same fate with different names and acronyms being used in numerous studies. In the current study the terminology of PFOS and the relevant isomers are adopted from a study by Chu & Letcher (2009) and the presented terminology has since been vastly used in studies to this date. An example of the acronym described relative to the name of its associated isomer is described in figure 1.

P3MHpS

Perfluoro-3-methylheptane sulfonic acid

Figure 1: Acronym and name of one of the branched PFOS isomer relevant to this study

Physical and chemical properties

The physicochemical properties of PFAS derives from the strong bond between carbon (C) and fluorine (F). Fluorine has the highest electronegativity among all atoms and makes one of the strongest covalent bond (C-F bond) with carbon in organic chemistry. The C-F bond makes the PFAS group thermally and chemically stable. The C-F bond is shorter than most covalent bonds with a length of 0.72 Å. For reference the length of a covalent carbon-carbon single bond is 1.5 Å. The densely packed shorter C-F bond with high electronegativity works as a shield against external attacks, which gives PFAS its persistent nature because of the strengthened thermal, photolytic, chemical, and biological stability. One of the most sought-after qualities of PFAS is its amphiphilic properties, which means that it has both hydrophobic- and lipophobic properties. The amphiphilic properties of PFAS derives from the low polarization in fluorine that gives weak intermolecular forces with both polar and nonpolar molecules. (Beuthe et al., 2016; Rayne & Forest, 2009)

PFAS generally low reactivity and great stability is one of the main reasons to their appliance in a broad specter of products. In textile, leather, and paper products, PFAS are used as surfactants because of their amphiphilic properties. PFAS is also used as surfactants to prevent corrosion of metal and are used in machines to prevent mechanical wear. The hydrophobic and lipophobic surfactant properties occurs only if the PFAS is paired with a hydrophilic functional group such as PFOS. PFAAs have a strong acidity due to the high electronegativity, which means that they occur exclusively in ionized form in nature. With the vast area of use, PFAS occurs in industrial sectors such as the aerospace, construction, and electronics industries. People are also exposed to PFAS as it is in multiple household items, such as non-stick cookware and food wrapping, but also in stain-resistant clothes and furniture. Exposure from the environment can also occur both directly and indirectly through food such as fish and vegetables. (Glenn et al., 2021; Kissa, 2001; Sunderland et al., 2019)

Synthesis

There are two main production processes of PFAS, telomerization and electrochemical fluorination (ECF) which is used for introducing perfluoroalkyl moieties into organic compounds. Telomerization is a process where a perfluoroalkyl iodide, most commonly pentafluoro ethyl iodide (C_2F_5I), reacts with tetrafluoroethylene to make longer chained perfluoroalkyl iodides. This process makes almost exclusively linear isomers. The other main production process, that also is the most applied is ECF. ECF is a process that uses an organic raw material, in the case of the chemicals in this paper; octane sulfonyl fluoride ($C8H_{17}FSO_2$, a derivate for PFOS) which undergoes electrolysis in anhydrous hydrofluoric acid (HF). This process leads to a complete replacement of hydrogen atoms with fluorine atoms. In addition of making linear PFOS, branched perfluorinated isomers and homologues are created. This is because of the free-radical nature of ECF, which leads to rearrangement and breakage of the carbon chain. The amount of desired linear isomers PFOS is roughly 70%. (Benskin et al., 2010; Buck et al., 2011). The products of technical PFOS from the main production processes with their distribution in water and ground is presented in figure 1-1.

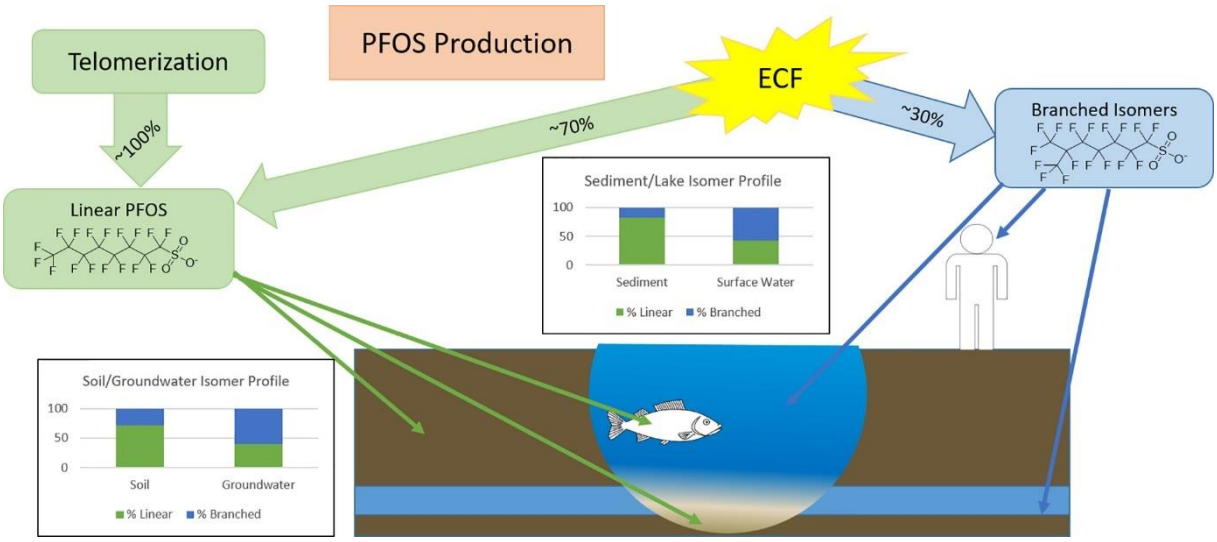

Figure 1-1 The technical product from the two main production processes. With its distribution in the aquatic environment. Reprinted with permission form Elsevier

Transportation

A study by Schulz, K. et. al. 2020 showed that branched isomers have a different distribution pattern than linear PFOS. Research suggests that branched isomers are more likely to remain in water, while L-PFOS preferably sorbs to soil and sediments. The ratio between L-PFOS and Br-PFOS in waters throughout the world varies widely from country to country and rarely fits isomer ratio of approximately 70% L-PFOS and 30% Br-PFOS by ECF. Multiple studies analyzing water samples; deviate from the ratio in T-PFOS from ECF either in favor of L-PFOS, or in most cases Br-PFOS (Ahrens et al., 2018; Chen et al., 2018). The reason behind this is the higher polarity of the branched isomers, which makes it less prone to adsorb to soil and sediments. Br-PFOS have been found in humans at higher percentages than what is produced by ECF, indicating that branched isomers affect the body differently. Some studies have found hazardous effects related to specific isomeric structures (Schulz et al., 2020).

As mentioned, roughly 20 to 30% of PFOS produced with the ECF process is branched (Buck et al., 2011), yet the amount of branched isomers found in human serum seems to exceed this limit. The ratio between linear PFOS and Br-PFOS in human serum varies from 58 to 70%. This means that Br-PFOS have a slight preferential accumulation in comparison with its linear counterpart (Karrman et al., 2007). Although wild animals seem to have a slight preferential accumulation to linear PFOS (Schulz et al., 2020).

Toxicology and regulations

There is a series of possible health risks linked to PFOS, but more research must be done. There are still indications of its toxicological properties. In 2002 The United Nations Organization of Economic Corporation and Development (OECD) released a hazard assessment for PFOS, which said that PFOS caused liver and thyroid cancer in rats and found an epidemiological link to bladder cancer in humans (OECD, 2002). Since then, more links to various cancers has been found, with the most consistent link between PFOS exposure and incidents of testicular and kidney cancer. More studies have also shown a link in breast, bladder and prostate cancer (Schulz et al., 2020). There are also epidemiological links that PFOS has metabolic effects, with the biggest correlation in hyperlipidemia, which is elevated cholesterol levels, but also increased body mass index (BMI) and impaired glucose metabolism.

PFOS are also linked to impaired thyroid function and infertility (Saikat et al., 2013). Multiple studies have shown a correlation between PFOS exposure and impaired immune system in children as well as neuropsychological diseases and obesity in children exposed to PFOS. There is also proof of a link between PFOS and cancer, though this is only in sites with extreme exposure (Braun, 2017; Sunderland et al., 2019).

In cases where health effects of L-PFOS and Br-PFOS have been studied separately, a different impact has been found. This can be seen in the prevalence of hypertension where one study found that the odds ratio of Br-PFOS to be higher at 1.26 (95% confidence interval [CI] 1.12, 1.42) compared to 1.11 (95% CI 0.97, 1.27) for L-PFOS. In some studies, specific health problems have been associated exclusively with Br-PFOS. Br-PFOS, but not L-PFOS, has been associated with decreased serum globulin and increased alanine transferase (ALT) levels with a 33% (95% CI 5.0%, 67.0%) increase in odds of having abnormal ALT levels (Schulz et al., 2020).

With the emerging international concern about PFAS persistency in the environment in the 2000's, many major manufacturers such as 3M and DuPont, phased out their production of PFOS. The phaseout resulted in a decreased level of PFOS (80%) in the bloodstream of Americans, showing that a phaseout was effective on human exposure (Brennan et al., 2021; Crinnion, 2010). The phaseout of multiple PFAS products resulted in alternative PFAS replacements such as perfluoro butane sulphonate (PFBS). PFBS was used because it gets eliminated from the body faster than the long chained predecessors, due to its shorter carbon chain (Conder et al., 2008).

The regulation of harmful and potentially harmful PFAS varies between international bodies, individual countries, and local areas. There are no consistent regulatory standards, and there is no agreement on the appropriate level of regulation.

In 2009 during the 4th Stockholm convention on persistent organic pollutants at Conference of the parties (COP-4) agreed to end the production and use of PFOS by adding it on the list for POPs with a few exemptions (Wang et al., 2009). During COP-9 the exemptions on PFOS was removed. Currently, 152 countries, both developed and developing countries, have ratified the Stockholm convention. There is still a problem with the regulation of PFAS among some of the signatories (Brennan et al., 2021). China is one of the signatories but is still the largest producers and consumers of PFAS (Chen et al., 2009). Even though the production of PFOS was limited in 2011, some countries still produce and distribute PFOS

chemicals. China still allows the use of PFOS in AFFFs, which is one of the major contamination sources of PFOS. Brazil still allows the use of pesticides containing PFAS that breaks down to PFOS (Brennan et al., 2021).

Environmental impact

In the 1970s PFAS was found in the blood of workers because of occupational exposure, in the 1990s PFAS was found in the general population. It was these incidents that raised awareness of PFOS as an environmental toxin as this was the most produced PFAS component (Buck et al., 2011). PFAA has been shown to bind to blood proteins in animals (Olsen et al., 2003). PFASs generally have a long half-life due to their physical and chemical properties, and PFOS have a half-life of 8.5 years in human blood which shows the chemicals environmental persistency (Olsen et al., 2007).

Although it was certain that there was PFAS contamination in the environment, PFAS was not as well documented because of analytical limitations due to the properties of PFAS and low concentrations. After 50 years of largescale production of PFAS chemicals, the first quantitative data came from environmental samples. A scientific article created by Giesy, J. P. & Kannan, K. in 2001, was the first large-scale publication on the quantification of PFOS in environmental samples. The analysis was performed on tissues from various marine mammals in both urban and rural areas such as the Arctic. This article concluded that PFOS was widespread in the environment. PFOS was found in animals near urban areas, but also in animals in remote areas. The finding gave an indication that PFAAs are bio accumulative. (Giesy & Kannan, 2001)

Not long after PFAA was found in tissue samples, PFAA components were detected in water samples, soil samples and sediment samples in areas far away where the chemicals were initially produced and used (Higgins & Luthy, 2006; Yamashita et al., 2005). In the arctics, where there often is the least amount of human influence, traces of PFOS among other PFAA compounds has been detected in abiotic samples, such as sea water and soil and in biotic samples such as marine animals and fish. When PFAA was detected in several stages in biotopes, it was clear that there must be a bioaccumulation of PFAA in the food chain (Benskin et al., 2012; Kowalczyk et al., 2020).

Bioaccumulation

Research of various PFAS components has been done on both animals and plants. PFAA and other PFAS components has been detected in every ocean in the world. Fish in most marine environments is under constant exposure to various PFAS components, even if this is a low concentration, this will further accumulate in the food chain. PFASs particularly long half-life means that it is persistent in both the environment and in animals, which is the main reason for its bio accumulative ability (Kissa, 2001). This is well emphasized by the fact that a correlation between the age of certain animals and the amount of PFAS found (Houde et al., 2006). In comparison between the bio accumulative abilities of PFAS and other POPs, it is less predictable to find the bio accumulative potential in PFAS due to its amphiphilic abilities, whereas lipophilic POPs can have a partition coefficient between polar and nonpolar solutions (Karrman et al., 2007).

PFAS components have been detected in all levels in the marine food chain and several hundred PFAS components have been detected in environmental samples. It is the bioaccumulation of these chemicals that is one of the driving forces for the exposure of PFAS (Sunderland et al., 2019). For every level in the food chain that is exposed, there is a biomagnification, which means that animals at the top of the food chain have significantly more environmental toxins than those at the bottom. If PFAS is detected at the lower part of the food chain, it is expected that the concentration raises for each stage (Houde et al., 2006).

In the marine environment at Svalbard, Norway, PFOS has been analyzed in both abiotic and biotic samples. A recent study from Svalbard did a largescale screening of multiple compounds in the PFAS family including PFAAs. The study concluded that there is an increasing amount of PFAS further up in the food chain. This biomagnification was shown, for example in the sum of the total PFAS concentration in the liver of fish and seagulls, which was 5.4 ± 0.87 µg kg-1 ww (wet weight) and 62.2 ± 11.2 µg kg-1 ww respectively where the majority of PFAS came from PFOS. (Ali et al., 2021)

Since the discovery PFOS in the environment in the early 2000s, there has been an emerging concern around other PFAS-components. PFOS replacements has been detected in the environment, the most prominent are perfluorobutane sulfonate (PFBS) and 6:2 fluorotelomer sulfonate(6:2 FTS) (Ali et al., 2021). With all the different PFAS components that are made and its isomers it is necessary to test further PFAS chemicals in the environment, especially because of PFAS persistent nature.

Isomer specific analysis

The first isomer-specific quantitation of PFOS were conducted using F^{19} NMR spectroscopy in 1997 to figure out the amount of linear and branched PFOS synthesized with ECF. In addition it gave a distribution profile between the Br-PFOS isomers present in T-PFOS by ECF (Company, 1997). The exact distribution of the different PFOS isomers varies among papers, the first study points to P2MHpS to be the most dominant product of ECF with approximately 58% of the Br-PFOS. A study by Arsenault et. al. in 2008 concluded P6MhpS to be the most abundant among the Br-PFOS isomers at approximately 31% using F^{19} NMR spectroscopy (Arsenault et al., 2008). In addition to P2MHpS, there are other technical products such as P44MHpS not present in this current study due to them not being available on the market.

Isomeric separation of Br-PFOS using gas chromatography (GC) has shown to be efficient at separating the isomers, but derivatization of the compounds must be done prior to GC-separation. The derivatization is done to make the PFOS volatile as PFOS generally are non-volatile. A paper made by Langlois et. al. 2007 derived L-PFOS and Br-PFOS using isopropanol to convert it to an iso-propyl ester under acidic conditions and managed to separate 11 PFOS isomers present in T-PFOS created with ECF.

The use of liquid chromatography (LC) is preferable to analyze trace amount of PFOS, as it is more efficient because no derivatization step is needed, which gives LC better sensitivity compared to GC. Today most PFOS analysis are done through LC analysis while volatile PFAS compounds are analyzed using both. In multiple studies, structure isomers of PFOS have been analyzed, but due to poor separation of these isomers using LC they all get categorized as Br-PFOS and is often summed up as the total amount of PFOS.

Aim of this study

The aim of this study is to develop an isomer specific method that are capable of separation and quantification of all L-PFOS and Br-PFOS isomers using a high-performance liquid chromatography tandem mass spectroscopy (HPLC-MSMS) apparatus, with the use of an ACE excel C18-PentaFluoroPhenyl (PFP) column. The selectivity of the method will then be compared with a reference method, which used a perfluorinated C_8 column, developed on the same HPLC-MS/MS instrument. Both columns have a higher selectivity towards halogenated compounds due to the fluorinated stationary phase. Most studies have shown that a fluorinated column yields better separation of PFAS and generally halogenated compounds

than the conventional C_{18} column, due to selective interactions. Per fluorinated C_8 columns are usually expensive and has a shorter lifespan compared to a C_{18} column. With the excessive cost and reduced durability of perfluorinated C_8 columns, these columns are mostly used in the scientific community but not in the industrial sector.

The analytical method utilizing the Ace Excel C_{18}-PFP column will be developed with the intention of analyzing L-PFOS and Br-PFOSs in environmental water samples. To test the methods ability to detect and quantify the target analytes, water samples from a lake near an airport and a river in a densely populated area were collected. The developed method will undergo a method validation were linearity, recovery, precision et cetera will be tested. Environmental samples that have previously been quantified and have a high amount of L-PFOS will also be tested to see if the developed method can quantify the target isomers in addition to making an isomer profile from the PFOS present in the sample. Based on calculated concentrations from each study site an isomer profile will be created to see the contribution of each isomer to the total amount of PFOS.

The HPLC- and MS/MS parameters were directly adopted from a study made on the same instrument (Skaar et. Al. 2019), but an optimalization of collision energy and fragmentation energy for each isomer will be attempted. Since Br-PFOS are structure isomers they all have the exact same mass of (499 m/z) and yields mostly the same fragmentations. This makes a good separation of the Br-PFOS crucial to achieve good reliable quantification of all isomers. With the previous method having a constant fragmentation energy and collision energy (CE), an optimalization of these instrument specific variables should achieve a better sensitivity than the existing method and might result in a better separation overall.

2. Materials and methods

Chemicals and reagents

A complete overview of all standards, reagents and materials is presented in appendix B. All chemicals were of HPLC grade.

0.1% Ammonia (NH_3) in methanol (MeOH) was prepared by diluting 1 mL of 25% ammonium hydroxide with 249 mL MeOH in a 250 mL volumetric flask

25 mM Acetate buffer with a pH of 4.5 was prepared by weighing 461 mg of Sodium acetate and 412 mg Acetic acid and transferring it to a volumetric flask and diluted with Milli Q water to a volume of 500 mL. The pH of the buffer solution was confirmed using a pH strip.

2 mM Ammonium acetate (NH_4Ac) in MeOH was prepared by adding 77 mg $NH_4Ac(s)$ to a volumetric flask and diluted with MeOH to a volume of 500 mL.

2 mM Ammonium acetate (NH_4Ac) in water was prepared by adding 77 mg $NH_4Ac(s)$ to a volumetric flask and diluted with Milli Q water to a volume of 500 mL.

The intern standard and all the standard solutions of branched and linear PFOS isomers were purchased from Wellington Laboratories (Guelph, ON, Canada). All isomers arrived in separate vials except for P45DMHxS and P35DMHxS. The initial concentration of the standards was 1 µg/mL except for P35DMHxS with 0.5 µg/mL.

Band broadening

The principle of chromatography is to separate molecules in a mixed sample by moving the sample with a mobile phase through a stationary phase, which causes a separation based on the different affinity each molecule has to the phases. In the case of HPLC, the mobile phase is a liquid, and the stationary phase is the particles in the columns. When the molecules are separated and gets detected in the tandem mass spectrometry (MS/MS) all the identical molecules do not come out at the same time. This is due to band broadening. Band broadening can be described as a measure of a column's efficiency. The efficiency of a colum can be described with the Van Deemters equation (2-1)

Equation 2-1: $$H = A + \frac{B}{u} + Cu$$

The *H* term is described as the Height Equivalent to a Theoretical Plate (HETP). Ideally the HETP of a column should be as low as possible to yield as narrow peaks as possible which results in greater selectivity. The *u* term describes the flowrate of the method. The *A* term describes Eddy diffusion and describes the number of pathways a molecule can travel. Eddy diffusion is most relevant to packed columns as there are particles the mobile phase must flow through. To minimize the effect of Eddy diffusion on the HETP, the particles in the column should be as small as possible. The *B* term is longitudinal diffusion and describes the diffusion of individual analyte molecules in the mobile phase along the axis of the column. This is due to the molecules tendency to move from an area of high concentration to an area with lower concentration. To reduce the impact of longitudinal diffusion on the HETP the mobile phase can be more viscous or increase the flowrate. The last term, the *C* term, describes mass transfer which deals with the sorption and desorption of analyte in the stationary phase.

The ACE Excel C18-PFP column was chosen with the Van Deemters equation in mind in regards of particle size and its interactions with the target analytes. When comparing the C18-PFP column and the per fluorinated C_8 columns, both have selective interactions with fluorine. The C18-PFP might not interact as greatly as the perfluorinated C8 columns on the premise of abundance of halogens in the stationary phase, but the C18-PFP column still have better separation compared to a regular C18 column. The Ace Excel C18-PFP column is good

at separating halogenated structure isomers to separate structure isomers according to the manufacturers.

Chromatographic method development

No studies using the ACE excel C18-PFP column for the separation of isomers were found, and the gradient program had to be made from scratch by initially using a scouting gradient. The other chromatographic parameters were directly adopted from the reference method, with the only difference being a lower injection volume from 10 µL to 5 µL to reduce band broadening. The full list of chromatographic parameters is presented in appendix D.

A chromatographic method using the ACE Excel C18-PFP column were developed by analyzing a mix of all the relevant PFOS isomers (table 1-1) through a scouting gradient. A scouting gradient was used to determine the strength of the B solvent to achieve separation. For reverse phase gradient it is most usual to use 100% acetonitrile as the composition of the B mobile phase, but due to accessibility 100% MeOH were used instead. The scouting gradient were conducted by having a gradient from 0% to 100% B over the course of 20 minutes. When the first peak eluted the composition of B was 56%. This gave an indication on the initial mobile phase composition when developing the gradient for the method. Because of the similarities in structure and affinity to the column, the standard mix were injected in isocratic conditions for 8 min at 50% B with the intention that the standards would spend more time in the column and thus achieve a better separation of the isomers all together. After the scouting gradient test, the steepness of the gradient was tested until a satisfactory separation and response of the isomers was acquired. All target isomers came in separate vials, except P45DMHxS and P35DMHxS.

The reference method uses an Epic FO LB column (1.8 µm, 120 Å, 2.1 mm × 150 mm, ES Industries) for separation. As mentioned, the reference method was heavily influenced by a paper made by Zhang et al. in 2018, which yielded an isomeric separation of all the branched PFOS isomers involved in this thesis using a Ultra-High-Performance Liquid Chromatography (UHPLC) instrument. The reference method did not share the isomeric separation of Br-PFOS as done in the method by Zhang et al. 2018.

Fragmentation and Optimalization

Since the Br-PFOS in this paper are structure isomers of their linear counterparts, the fragmentation pattern is almost identical. The product ions made during fragmentation consists mostly of 0-series and 9-series fragments. The 0-series fragments usually mean loss of one or more fluorinated carbon in the alkyl group, while 9-series fragments usually describe the loss of the sulphonate functional group in addition of fluorinated carbons.

The optimalization of the Multiple reaction monitoring (MRM) transition were first adopted by the reference method by evaluating the possible fragments using a constant collision energy (CE) of 61 eV and a fragmentation energy of 200 V. The initial MRM transitions were adapted from the previous method, but different product ions were tested to find the optimal MRM transitions in regards of response strength. The tested product ions are shown in table 2. To improve the transitions of each target analyte, a CE-range from 0 to 100 eV with increments of 10 were applied on all MRM transitions. The fragment energy of 200 V was

kept during this stage of optimalization. If the response was higher at 100 eV, further levels of CEs were tested. The quantifier ion and qualifier ion for each target analyte, were decided based on the strongest signal of each product ion. The CE of each transition were then optimized by running triplicates with ± 10 eV of the initial CE. A similar procedure was conducted when optimizing the fragment energy, where a range between 100 and 240 V with an increment of 20 V were tested. It was expected that the CE would have the greatest impact on response strength. The internal standard used in this study was not optimized as tests showed that the added internal standard gave a sufficient response.

Table 2: The product ions tested on each isomer		
Fragment series	Structure	Product ions (*m/z*)
0-series	$C_mD_{2m}SO_3^-$ $1 \leq m \leq 7$	130, 180, 230, 280, 330, 380, 430
9-series	C_nF_{2n+1}	69, 119, 169, 219, 269, 319, 369, 419
Other	FSO_3^- SO_3^-	99 80

Study sites and sampling location

Two different study sites were chosen when sampling, one with a possible direct source of contamination and another with multiple sources of contamination. Both sampling locations have a possibility of being contaminated through AFFFs from airports. One field blank was taken for both sampling locations.

Kjeller airport (N 59°97’, E 11°04’) is located in Lillestrøm municipality. Kjeller airport was made in 1912 for the Norwegian Army Air Service. This was the first airport in Norway and is one of the oldest airports still operating. At the start of World War I in 1914, the airport became subject to major expansion which in return gave higher military capacity. The use of PFAS containing AFFFs has been confirmed used since the early 1970s, but cases where the foam has been used to put down fires is unknown (Forsvarsbygg, 2017).

A small lake near Kjeller airport called Sogna was chosen as sampling location as it is within short perimeter of firefighting training sites at the airport as shown in figure 2. A report by Forsvarsbygg in 2017 detected high levels of PFOS close to the fire-fighting training sites with concentrations ranging from 590 to 62 ng/L. The sampling location had drainage pipes that ran directly into sogna, which might give a lower amount of detected PFOS. A picture of the drainage pipes is found in appendix I.

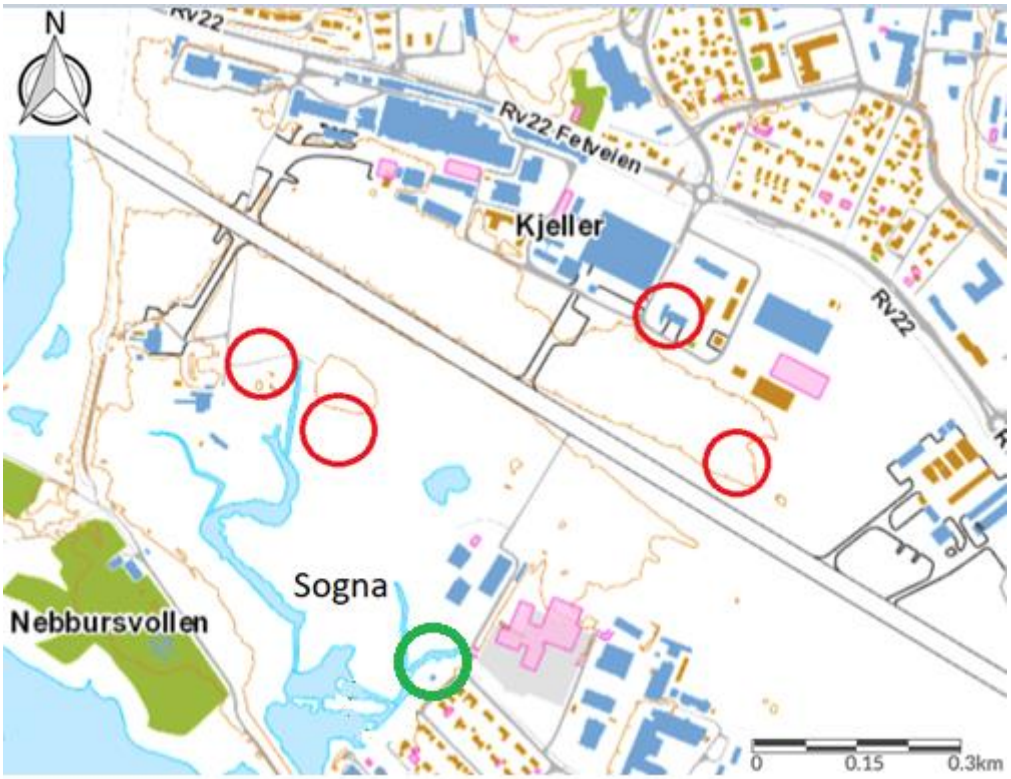

Figure 2: Map depicting Kjeller airport with sampling location for this current study (green) and locations of past and present fire-fighting training sites at Kjeller airport where AFFFs might have been used (red). The locations of the fire-fighting training sites were first published in a paper by Forsvarsbygg in 2017. The map is from norgeskart.no.

Fjellhamardammen (N 59°94', E 10°99') is a pond connected to Fjellhamar river in Lørenskog municipality that runs from a lake called Langvannet. The pond is part of an environmental park. Langvannet is located in a densely populated area and is exposed to pollution from industrial sites, households and has possible sites of AFFF contamination from fire-fighting training sites. There are no documented cases of PFOS quantitation in fjellhamar river or Langvannet, so this will provide insight in the presence of PFOS.

Figure 3: Map depicting Fjellhamardammen with sampling location (green). The map is from norgeskart.no.

A pre-prepared sample from runoff water in Ny-Ålesund (N78.9285 E11.91476) was also chosen with a high level of L-PFOS and with Br-PFOS present. This lake lies within close proximity of a fire-fighting training site that have used AFFFs containing PFOS. The map of the sampling location is found in figure 4 in addition to the location of the fire-fighting training site. The sample was used in a previous study by Skaar et. al. in 2019 to map the PFAS composition profile. The study calculated a total sum of PFOS involving L-PFOS and Br-PFOS. The total concentration of PFOS was determined in the mentioned study to be 310 ng/L. (Skaar et al., 2019)

Figure 4: Sampling location (green) for the sample from Ny-Ålesund and the location of a firefighting training site (red). (Source: google maps)

Sample collection

The samples were collected approximately 0.5 meters below the water surface using a 1 L polypropylene container free of PFAS. Three samples were collected from each sampling location to assure better precision.

Transport and storage

The samples and field blank were transported directly to the Faculty of Veterinary Medicine (VET) at NMBU in Ås the same day the samples were collected. To prevent contamination, the samples were stored in a case with a tightly closed lid until its arrival. The samples were stored in a fridge with a temperature of 5°C until the sample preparation procedure.

Sample preparation

The sample preparation procedure was conducted in its entirety at the Faculty of Veterinary Medicine (VET) at NMBU in Ås. To prevent contamination of the samples and blanks, all equipment was free of PFAS. The samples were never in contact with any glass, as PFOS tends to sorb to glass which would result in loss of analyte. 50 uL of 200 ng/mL intern standard (ISTD) was added to each sample and blank prior to the sample preparation, to

correct for any possible loss of analyte. The sample from Ny-Ålesund went through the exact same extraction procedure.

SPE WAX extraction

Samples of water were extracted by solid-phase extraction (SPE) with a mixed mode reverse phase/weak anion exchange (WAX) resin to isolate the L-PFOS/Br-PFOS anions through interactions with cations in the WAX sorbent. Extraction was achieved using a Waters Oasis® WAX (500 mg, 6 cc, 60 µm, Waters, Milford MA, USA) that was conditioned with 4 mL 0.1% NH_3 in MeOH followed by 4 mL MeOH and finally 4 mL Milli Q water. The SPE cartridges was attached to a vacuum manifold after conditioning and 4 mL of Milli Q water were added to prevent the resin from drying out during the sample loading. The samples were loaded to its respective SPE cartridge through silicone tubes. All replicate samples were extracted at the same time.

The loading speed of the sample was approximately 1-3 drops per second, which constitutes to maximum 5 mL/min. The loading time for a 1 L sample of freshwater was 5-12 hours. The cartridges were then cleaned using 4 mL 25 mM acetate buffer to remove salts and other interferences as well as improving adsorption of target analytes to the sorbent. The now cleaned cartridges were then centrifuged at 1500 rpm for 2 minutes to remove residual solvents. Prior to the extraction of PFOS, the SPE cartridges was washed with 4 mL methanol which further cleaned the resin and extracted nonionic PFAS from the resin. To extract the potentially collected PFOS, 4 mL 0,1% ammonia (NH_3) in methanol were added to the cartridges and were collected in individual 15 mL propylene tubes. The flowchart of the method is presented in appendix C.

Evaporation and Filtering

After extraction, the samples were dried by compressed air evaporation at 60°C until complete dryness and resolved with 500 µL methanol (MeOH). To assure that all target analytes were resolved, each polypropylene tube were vortex mixed for 60 seconds and was left to sit for 30 minutes and then vortex mixed again for 60 minutes before filtering.

Prior to analysis each sample were filtered using a spin-x vial and centrifuged at 12 500 rpm for 3 minutes. The filter was then disposed, and the samples were transferred to new LC-vials for HPLC analysis. This were done to remove any particles in the samples to not damage the HPLC-MS/MS system.

Instrumental analysis

The instrumental method development, validation and analysis were conducted at the faculty of Veterinary Medicine (VET) at NMBU in Ås, Norway.

The separation of target analytes in samples and standards was conducted on an Agilent 1200 HPLC system coupled to an Agilent 6460 Triple quadrupole (QqQ) mass analyzer (MS/MS). An ACE C18-PFP column was used for the isomer specific chromatographic separation.

HPLC separation and identification of analyte isomers

The HPLC-MS/MS analysis were conducted at the Faculty of Veterinary Medicine (VET) at NMBU in Ås. As the main goal of the study was to develop a method for isomer-specific HPLC-MS/MS PFOS determination, a resolution sufficient for quantitative analysis on all

target analytes was sought after. Regarding the target isomers structural similarities to each other they tend to have overlapping mass transitions. Therefore, it was favorable to achieve a complete isomeric separation to be able to quantify all target analytes.

Identification of the target isomers were done by injecting standards of each target analyte individually with a concentration of 25 ng/mL. The potential isomers in the freshwater samples could then be identified based on the retention time given by the result of each standard. The standards were analyzed during the same run as the freshwater samples to assure corresponding retention times with the target analytes in the samples.

Table 2.1 The gradient program for HPLC separation. Mobile phase A was 10 % MeOH in water (v/v) with 2 mM NH4Ac and Mobile phase B was 100 MeOH with 2 mM NH4Ac.

Time (min)	A (%)	B (%)
0	50	50
8	50	50
15	15	85
18	0	100
20	0	100
25	50	50

MS/MS detection and parameters

The target analytes were detected using an Agilent 6460 series triple quadrupole mass spectrometer after the chromatographic separation. The MRM-transitions are listed in the appendix D and were the determined and optimized transitions from the method development. The other MS-parameters are also presented in the appendix D.

Precautions and measures

Even though PFOS production has been largely phased out since the early 2000s, it is still a risk of PFOS contamination from imported products such as textiles and packaging from countries who still allows the use of PFOS. As PFOS is widespread in waters and soil all over the world, it poses a threat of contamination of samples during all stages of sample handling. Procedural- and instrument blanks were used to correct any possible contamination of the samples. All equipment used during the sample handling was free of any PFAS component, this includes but not exclusively, pipette tips, silicone tubes, PP canisters and tubes among other equipment. Any contact with the samples were done using nitrile gloves and sample collection were done using measures in regards of PFAS free clothing. The lab facilities required a change of shoes and the use of a lab coat prior to entering the lab facilities. During sample preparation the 1L containers of water were covered with a lid to prevent airborne contamination.

3. Method validation and quality assurance

The column used for chromatographic separation in this thesis has been used previously used for analyzing PFOS among other compounds. To reduce the possible contaminations from the column, the column was washed excessively with Milli Q water and pure methanol prior to the method development. During analysis blanks were used before, during and after analysis, to see if any interferences were detected. After each analysis the column went through a washing program to remove the ammonium acetate from the column between each analysis.

Traceability

To assure good traceability, each sample was given a sample code prior to extraction. The sample code for freshwater samples consisted of the sampling location in addition to the number of the replicate from the respective sampling location. Samples that were spiked with the target analytes were included in the sample code. During extraction, the sample code followed each step during the procedure. Field-, transport- and storage blanks were given a sample code describing what type of blank there was. Calibration standards and instrument blanks did not get a sample code as they did not go through the sample procedure.

Selectivity

The International Union of Pure and Applied Chemistry (IUPAC) defines selectivity as “the extent to which other substances interfere with the determination of a substance to a given procedure.” Selectivity can therefore be described as the potential for an accurate and precise determination of the presence of an analyte among other components. This is an especially important analytical parameter in trace analysis, where the analyte is harder to distinguish among the interferences due to low concentrations. This parameter is usually the first parameter to be determined during the method validation process. There are factors that both improve and worsens the selectivity of a method.

The factors that afflict the selectivity negatively is

- The more unknown the sample composition
- The more complex the sample matrix
- The analyte shares the same properties as the matrix components
- The higher the amount of analytes
- Low analyte concentration
- The bigger the similarities between the analytes

As mentioned, the isomers in this paper share similarities with each other in regards of the molecular weight and the properties, as they are structure isomers of PFOS. This might affect the selectivity of each compound.

The selectivity can be improved by

- using selective analytical methods

- eliminating the impact of interferences by removing them or hiding them
- isolating the analyte from the matrix

Selectivity was determined by analyzing each target analyte individually and comparing them to a mix of all standards with a concentration of 10 ng/mL. The selectivity was then evaluated visually based on the separation among the standards. Selectivity was the determining factor when developing the LC method.

Linearity and linear range

Linear dependency is the most common parameter to use in analytical chemistry. To assess the linearity, a calibration curve containing a range of concentrations of the analytes were used. The concentration should span over the expected concentration of the analyte in samples. For each increase in concentration in the calibration curve there is a calibration step. A calibration step is the signal associated with the corresponding analyte concentration. The most regular way of testing linearity is with linear regression, which also can be used to evaluate the trueness, the limit of detection (LOD) and the limit of quantification (LOQ). To figure out the linearity, the standards solutions used must meet three requirements.

1. The expected analyte concentration in the samples is within the concentration range
2. Do not include more than three orders of magnitude of analyte concentrations
3. The concentrations of the standard solutions are evenly distributed within the concentration range

The linearity was evaluated using standard solutions for each PFOS isomer listed in table 1-1 with a concentration range of 50 ng/mL to 0.5 ng/mL with a total of six individual concentrations. The standards were run in three replicates on multiple reaction monitoring (MRM) and the mean value of the replicates were used to assess the linearity. The linearity criteria were a regression curve R^2-value of at least 0.99. A C13 marked Sodium perfluoro-1-[1,2,3,4-$^{13}C_4$] octanesulfonate (MPFOS) ISTD was added to each solution with a concentration of 20 ng/mL. A criterion of a R2-value of 0.99 proved that the concentration range of the target analytes can be measured linearly. The calibration curves were weighed in favor of lower concentrations.

Limit of detection (LOD) and Limit of quantitation (LOQ)

Limit of detection (LOD) describes the lowest concentration of analyte that with certainty can be detected in a method. Limit of quantitation (LOQ) is the lowest concentration that can be quantified in a method. Calculations of LOD and LOQ varies in literature, as there are many ways of calculating and defining them. The definition used in this study is a signal to noise ratio of 10 for LOQ and 3 for LOD.

LOD and LOQ were calculated by plotting the signal to noise ratio of each concentration from the calibration standards and then using linear regression to get a slope. The slope was then used to figure out the concentrations using equation 3-1 and 3-2 representing the LOD and LOQ, respectively.

Equation 3-1: $LOD = \frac{3}{slope}$

Equation 3-2: $LOQ = \frac{10}{slope}$

Quantification and data handling

To calculate the concentrations of the unknown samples the internal standard method was used to quantify the target isomers. This was accomplished by creating calibration curves for all target isomers with a concentration range between 0.5 to 50 ng/mL. All samples and standards that were analyzed got the same amount of ISTD. The calibration curves were created by plotting the ratio between the response of both target isomer and the respective ISTD at the y-axis and the respective concentration on the x-axis. A linear dependency was found using linear regression to get a calibration curve equation. The calibration curve and quantification were calculated automatically with Masshunter software version 10.1 (Agilent Technologies, Santa Clara, CA, USA). If coelution occurred among the target isomers, they were treated as one peak and would be quantified together.

Recovery

Recovery is a metric that refers to the ability of the method to give a response for the entire amount of analyte in a sample. This can be a measurement of any matrix effects from the samples, which can either be ion suppressing or ion reinforcing. The recovery was calculated using the calculated concentrations from all target analytes in spiked, unspiked and the actual concentration added. The concentrations were calculated based on the ratio between the response given by each concentration in the calibration curves and the respective internal standard response. Potential interferences from the sample matrixes were ruled out by using unspiked replicates of each spiked sample. The concentration of the added target analytes in the spiked sample were calculated by subtracting the peak area of unspiked samples from the respective sample replicate. The recovery tests were conducted on water samples from Fjellhamardammen environmental park. Eq. 3-3 was used to calculate the recovery.

Equation 3-3: $\%Recovery = \frac{c(spiked) - c(unspiked)}{c(added)}$

An acceptable recovery range was set between 40% to 120% as a criterion for the method validation. Any recovery outside this limit was deemed unacceptable for each target analyte.

Precision and accuracy and method uncertainty

Precision is a measurement that describes the analytical instrument's ability to give a consistent response to a sample with known concentration of the target analyte(s). The true precision is the mean value of an infinite number of replicates. In practice, precision is decided by analyzing the same solution containing the analyte(s) multiple times and then calculating the coefficient of variance CV% based on each analyte's response. The %CV was calculated using equation X.

Equation 3-4: $\%CV = \frac{Standard\ deviation\ of\ replicates}{Mean\ value\ of\ replicates} * 100$

Equation 3-5: $\%BIAS = \frac{C_{Calculated} - C_{True}}{C_{True}}$

This was accomplished by analyzing solutions containing intern standard and standards of each analyte in 5 replicates. The concentration of the analytes were 20 ng/mL intern standard and 25 ng/mL of the target analytes. %CV values below 30% were deemed acceptable, while values above 30% were deemed unacceptable. The accuracy was determined based on bias and are calculated based on the deviation of the calculated concentration of each sample relative to the true concentration as shown in equation 3-5. The same acceptable limit applies for the calculations of %BIAS. The calculations of precision and accuracy provides a measure of the uncertainty for each analysis.

4.Results

Method development

A complete isomeric separation was not achieved. The chromatographic method managed to individually separate the monomethylated P1MHpS and P6MHpS in addition to L-PFOS. The dimethylated isomers were not separated and coeluted in one peak of P45DMHxS, P35DMHxS and P55DMHxS. The rest of the monomethylated P3MHpS, P4MHpS and P5MHpS also coeluted in one peak. The separation is presented in figure 5.1with the target isomers assigned to their respective peak.

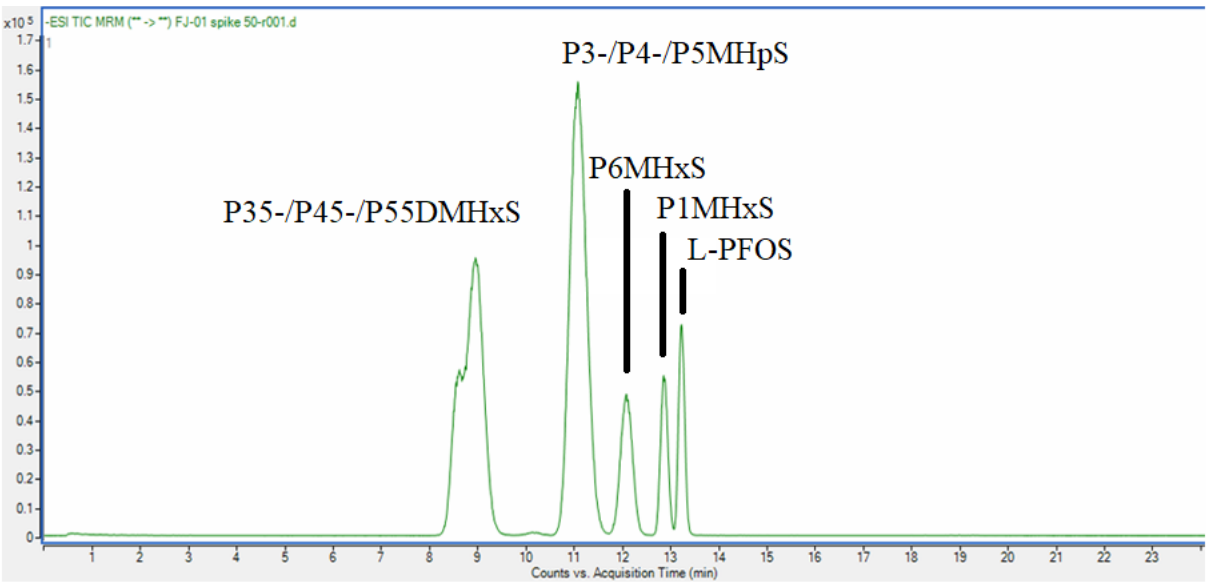

Figure 4.1 TIC Chromatogram of all target analytes showing the peaks and their respective isomer(s)

With similar product ions among the coeluting isomers, it was not possible to separate the isomers based on MRM-transitions. The Coeluting peaks was therefore treated as one peak and quantified using the optimized CE and fragmentation energy of the coeluting isomer that gave the best response. The optimization of the MRM-transitions gave an improved response for all target analytes compared to the constant CE and fragmentation of 61 eV and 200 V respectively. In some cases, the optimalization yielded a threefold improvement, but only some minor improvements occurred for certain MRM-transitions. Chromatograms depicting the increased response from the optimalization is presented in appendix E.

Findings

As presented in table 4.1, PFOS was detected at all study sites with L-PFOS dominating the isomer composition among the analytes. No samples from Fjellhamardammen or Sogna environmental park had a detectable concentration of P1MHpS. In both mentioned study sites, no P35-/P45-/P55DMHxS was detected either. The remaining analytes were at a quantifiable level in both Sogna and Fjellhamardammen environmental park. The samples from Sogna contains more L-PFOS compared to the samples from Fjellhamar as visualized in figure 4.2, with a concentration of 2,97 ng/mL and 2,53 ng/mL respectively.

The runoff water sample from Ny-Ålesund had a determined PFOS concentration significantly higher than the latter study sites with L-PFOS and P6MHpS being above the linear range of this method (table 4.1). The sample has concentrations for L-PFOS and P6MHpS above the linear range of this method with calculated concentrations of 319,83 ng/mL and 71,61 ng/mL respectively but was kept to get an estimated value for the isomer profile in each sample. The remaining target analytes was at a quantifiable level, including the coeluting P35-/P45-/P55DMHxS analyte. Figure 4.3 shows a chart over the calculated concentration of each target analyte in the sample from Ny-Ålesund.

Figure 4.4 Shows the isomer profile based on the contribution of each target isomer relative to the total amount of PFOS present in the samples. The P1MHpS for the samples from Fjellhamardammen environmental park was excluded due to the concentration being below the LOD but was kept in the samples from Sogna as it was detectable. The calibration curves for each target isomer are found in appendix F.

Table 4.1: Mean determined concentrations from each sample in ng/mL. Concentrations below the LOD is marked with red. Concentrations above the linear range is marked with green.

Analyte	FJ (n=3)	KJ (n=3)	NÅV (n=1)
P1MHpS	0,17	0,16	12,98
P6MHpS	0,84	0,84	71,61
P3-/P4-/P5MHpS	0,82	0,99	139,82
P35-/P45-/P55DMHxS	Not detected	Not detected	3,39
L-PFOS	2,54	2,97	319,83

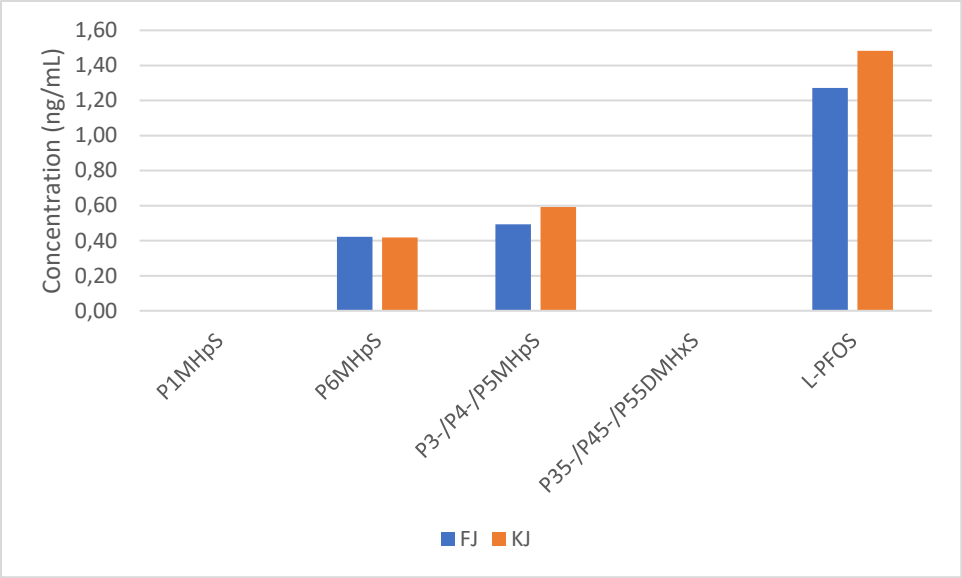

Figure 4.2: Chart overview of the mean concentration of each target analyte present in the watersamples from Fjellhamar river and Sogna

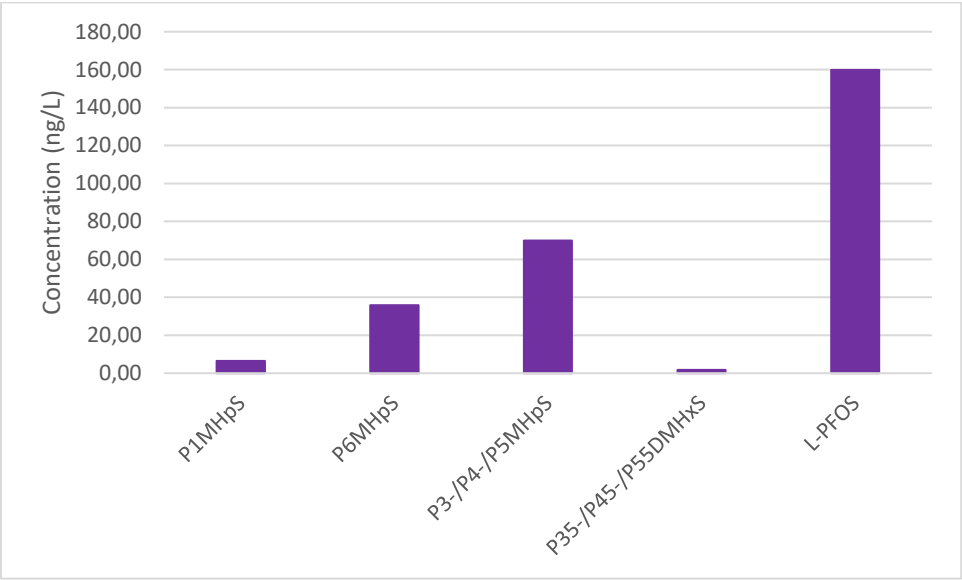

Figure 4.3: Chart overview of the determined concentrations (ng/L) of the target analytes in the water sample from Ny-Ålesund. Note that L-PFOS and P6MHpS are above the linear range of this method.

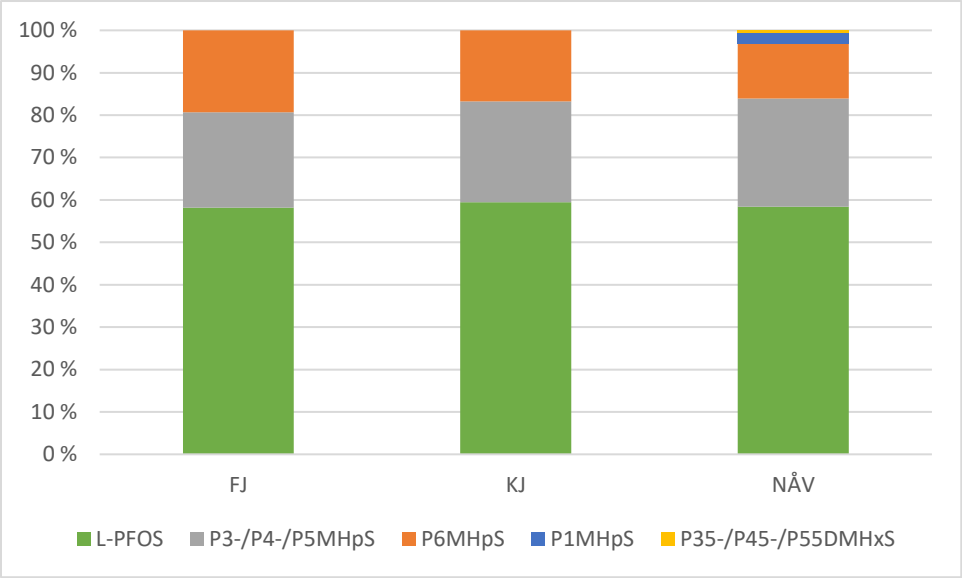

Figure 4.4: Isomer profile in present relative to the total PFOS among the detected analytes from each studysite.

Method validation and quality assurance

The linear range, R^2-value, LOD and LOQ is presented in table 4.2. The linearity requirements were within a satisfying range for all analytes, but the 50 ng/mL calibration step in P1MHpS and L-PFOS was left out to get a satisfactory R^2-value and thus resulted in a lower linear range from 0,5 to 40 ng/mL. It was assumed that the 50 ng/mL calibration step for said isomers was because of incorrect dilution. The lower end of the linear range was below the LOQ for P1MHpS, P6MHpS and P3-/P4-/P5MHpS calibration curves. The expanded range from the coeluting analytes is the result of 50 to 0,5 ng/mL being added of each standard to the calibration standards.

Since the linear range of P1MHpS and L-PFOS (0,5-40 ng) is below the highest concentration in the recovery test of 50 ng/mL, it was assumed that the calibration curve was linear at 50 ng/mL because the R^2-value was within the criterion for the calibration curves.

Table 4.3 presents the calculated recovery, precision shown as %CV and accuracy presented as %BIAS. The recovery of each target analyte was within the criteria of 40 to 120%. The branched isomers had a recovery between 90% to 98% while L-PFOS had a recovery of 73%. The calculated %CV of each target isomer ranged from 1% to 5% which fulfills the validation criterion of <30%. The calculated % BIAS was also within acceptable limits with a calculated % BIAS range from -14% to -1% and shows that the determined concentrations are expected to measure concentrations lower than the true concentration.

Table 4.2: Overview of the Linear Range, R^2-values, LOD and LOQ

Analyte	Linear Range (ng/mL)	R^2	LOD	LOQ
P1MHpS	0,5-40	0.999	0,26	0,87
P6MHpS	0,5-50	0.999	0,20	0,66
L-PFOS	0,5-40	0.995	0,11	0,37
P3-/P4-/P5MHpS	0,3-150	0.996	0,22	0,73
P35/P45-/ P55DMHpS	0,25-125	0.995	0,18	0,60

Table 4.3: Overview of the calculated %recovery for all target analytes and the calculated % coefficient of variation and %BIAS for all target isomers.				
Analyte	Mean % recovery	Mean Ccal (± SD)	%CV	%BIAS
P1MHpS	99 %	24,63 ± 0,25	1 %	-1 %
P6MHpS	98 %	23,10 ± 0,35	3 %	-8 %
L-PFOS	73 %	24,20 ± 0,55	2 %	-2 %
P3MHpS	90 %	21,52 ± 0,38	5 %	-14 %
P4MHpS		24,44 ± 0,35	1 %	-2 %
P5MHpS		23,38 ± 0,94	2 %	-6 %
P55DMHxS	90 %	24,66 ± 0,23	2 %	-1 %
P35-/P45DMHxS		24,30 ± 0,57	2 %	-3 %

No contamination or carry-over effect was found in the procedural blanks as well as instrumental blanks, thus no correction was needed on the samples. With no detected contamination from the procedural blanks proves that as far as the range of the method goes, no contamination occurred during sampling, transportation, storage, the sample preparation, and HPLC-MS/MS analysis. This signifies that the solvents, standards, reagents, mobile phases, and materials had no significant PFOS contamination. A selection of blank samples is presented in the appendix E.

5. Discussion

Isomer separation

Even though a complete separation of the target analytes was not achieved, a complete separation of L-PFOS, P1HpS and P6HpS gives the opportunity to determine the concentrations of them individually. A complete isomeric separation was not expected and not achieved, but the isolated P6MHpS-peak gives the opportunity to quantify the most abundant Br-PFOS isomer in T-PFOS by ECF according to the study by Arsenault et. al. 2008. The coeluted peaks of P1/P3/P5-MHpS and P35/P45/P55-DMHpS being treated as the same analyte, means that an accurate quantification of each coeluting isomer is not possible due to similar fragmentation patterns. The isomer profile of T-PFOS is presented in the paper by Arsenault et. al. 2008 can be used to get an estimated concentration if the source of PFOS originates exclusively from T-PFOS by ECF. As all study sites have a possibility of AFFF contamination, such an estimation can provide insight in each coeluting isomers individual concentration. The complete contribution of each PFOS isomer is presented in appendix A.

Table 4.2 and 4.3 shows that all method validation parameters were within the given criterions. There are some sensitivity issues regarding the fact that the lower range of the calibration curve is below the limit of quantification for all instances except L-PFOS. As all analytes achieved a R^2 value above 0.99, indicates that they are linear within the calibration range. As for the shorter range of P1MHpS and L-PFOS, linearity was assumed for the concentration of 50 ng/mL to be able to calclate the recovery of the spiked samples. The recovery sample had a real value of 50 ng/mL and both samples measured a similar concentration.

The precision and accuracy for the analytical method was within the validation criterions and gives the uncertainty for each measurement, but further concentrations at the higher and lower end of the calibration curve should be tested. The recovery of the spiked matrix sample represents both matrix effects and loss of analyte during sample preparation.

The coeluting peak containing the dimethylated isomers seems to contain two peaks. The result of analyzing pure P45DMHxS/P35DMHxS standard gives a coeluted peak, but based on the shape, some separation occurs between the mentioned isomers. It is not possible to identify the peak that represent its respective isomer. The other coeluting peak containing the monomethylated P3MHpS, P4MHpS and P5MHpS have no clear indications of separation within the peak. This means that they either have little or no difference in affinity to the column. The broader peaks of around 1 minute might be an indication that there are some differences in affinity to the column. The peak shape of the P1MHpS and P6MHpS branched isomers and L-PFOS seems to be symmetrical.

Overlapping occurred between the P1MHpS and L-PFOS peaks, but this was only a minor overlap. During method development there were attempts at improving the resolution by changing the mobile phase gradient program, but no further improvement was achieved. The resolution might be improved by changing the mobile phase solvents or pH. Based on the general shape of the peaks, the current method has no signs of tailing contrary to the reference method.

In comparison with the reference method that managed to separate P6MHpS and L-PFOS, the method developed in this study managed to separate the P1MHpS isomer in addition to L-PFOS and P6MHpS. When looking at the degree of separation, the current method has managed to clearly separate the peaks of the analytes. The chromatogram depicting the separation achieved from the reference method is presented in figure 6.1.

There are multiple factors that can affect the separation in a method such as mobile phase composition, temperature, and the dimension of the columns. As the reference method used a C8 perfluorinated column with a particle size of 1,8 µm in comparison with the current methods 3 µm, means that the C8 perfluorinated column have more surface area that the analytes can adsorb to and more pathways for the analyte. The cost of using smaller particles is a limited flowrate. Based on the HETP calculated from the Van Deemters equation, the C8 perfluorinated column should have better Eddy diffusion and mass transfer in regards to the lower particle size. What makes the Ace Excel C18-PFP favorable is the higher achieved flowrate of 400 mL/min in comparison with the reference methods 0,150 mL/min which in return gives an improved longitudinal diffusion. As the reference method was adapted from a method made for a UHPLC instrument, this strengthens the claim that the reference method was not fit for a HPLC instrument due to the lower achieved flowrate.

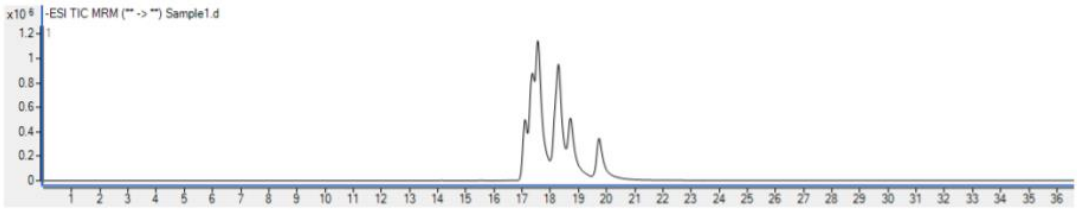

Figure 6-1: Separation of the target isomers achieved from the reference method (Lennikov, 2021).

Shifts in retention time for all peaks occurred during the sample run (appendix H). This is an indication that the column has not been properly equilibrated prior to and during the run. An increased re-equilibration time in the gradient program will likely solve this issue. The equilibration time in the gradient program was initially based on when the internal pressure of the binary pump was stable, but the shift in retention time indicates that it must be prolonged. Even with the shift in retention times the chromatograms yielded the same degree of separation which points to the methods robustness. The robustness of this method was also shown when developing the method, where different gradient programs were used, acceptable separation still occurred. Examples of chromatograms during the method development is presented in appendix E.

Findings

The detection of Br-PFOS proves that the study site has a contamination source of PFOS from T-PFOS by ECF and not telomerization which would give exclusively L-PFOS. Since not all PFOS isomers present in T-PFOS are included in this thesis, there are possibilities that the remaining isomers coelute with the target isomers. This will possibly influence the calculated concentrations of the target analytes in the freshwater samples and will result in false elevated concentrations of each analyte. Since there are no standards of the remaining PFOS isomers available on the market, there are no way of verifying where or if coelution occurs. The chromatograms from all study sites had no other visible peaks which makes the possibility of coelution likely. The possibility of coelution from non-identified PFOS isomers is an uncertainty in this method and affects the measured concentrations in the samples. This means that even though this method managed to separate the target isomers into 5 peaks whereas 3 was totally separated, it is uncertain if these target analytes were quantified exclusively in the environmental samples.

The P35-/P45-/P55DMHxS was not detected in any of the samples from Fjellhamardammen environmental park and Sogna. The sample from Ny-Ålesund contains a significantly higher amount of PFOS compared to the samples from Fjellhamardammen environmental park and Sogna. This made it possible to quantify the P35-/P45-/P55DMHxS which in total contributes to 0,81 % of the isomers present in T-PFOS. Since the amount of L-PFOS in the other study sites had concentrations below 3 ng/mL, a detection of the dimethylated Br-PFOS or the P1MHpS analyte was not expected.

An uncertainty to this method is the usage of the M4PFOS ISTD which is a linear ^{13}C-marked PFOS. As mentioned in the introduction, the Br-PFOS have a higher polarity due to the fluorinated methyl-groups which makes them less prone to sorption on sediments and soil. This means that loss of ISTD during extraction might not correlate with the loss of Br-PFOS during sample preparation. This might lead to less accurate quantitation of the branched

isomers, which is an uncertainty in this method. The less accurate quantitation might give incorrect recovery calculations of the target branched isomers. Unfortunately, there are no ^{13}C marked Br-PFOS available on the market. The ISTD might not be optimal for quantifying Br-PFOS, but based on availability on the market, the chosen ISTD was optimal. The use of a ^{13}C- Perfluoroheptanesulfonic acid (PFHpS) as ISTD might be interesting to try because of the shared heptyl-chain structure with the monomethylated PFOS isomers. Nevertheless, it will still be in linear form with the same problem that applies to M4PFOS.

Another reason for the difference in recovery between L-PFOS and Br-PFOS might be because Br-PFOS is easier to extract from the water matrix compared to L-PFOS. Loss of analyte can occur during the sample preparation process due to sorption on surfaces. This is another factor to consider when comparing the recoveries of L-PFOS (73%) and Br-PFOS (90-98%). The calculated recovery might also be affected by other PFOS isomers present in T-PFOS by ECF coeluting along with the target analytes which gives an overcorrection from the unspiked samples.

The isomer profile presented in figure 4.4 from all environmental samples provides insight in the different behavior between Br-PFOS and L-PFOS in aquatic environments. Based on the contribution of L-PFOS relative to the total PFOS, all samples had less than 70% contribution. This means that the amount of PFOS present in the freshwater samples deviate from the contribution of L-PFOS in the technical product by ECF. Even though P2MHpS and P44MHpS is not quantified in this paper, their impact on the concentration calculation is a possibility. The deviating distribution of PFOS isomers from T-PFOS fit the tendency of L-PFOS preferential sorption to soil and sediments, in addition to Br-PFOS elevated affinity to stay in water. The ratio among the isomers in the coeluting monomethylated peak is 32,8%, 26,8% and 40,4% for P3MHpS, P4MHpS and P5MHpS respectively. This constituted a concentration of 45,86, 37,47 and 56,48 ng/mL for the samples from Ny-Ålesund.

None of the study sites have determined the isomer profiles of PFOS, so the only comparison can be done through the total amount of PFOS determined with the analytical method.

The determined concentration of total PFOS in the samples from Fjellhamardammen environmental park at 2,19 ng/L. As there are no literature on the measurement of PFOS in either fjellhamar river or Langvannet more samples need to be taken in order to map the amount of PFOS upstream and downstream of the river. It was expected to find high concentrations of PFOS from the samples form Sogna as the report from Forsvarsbygg in 2017 determined a range from 62 to 590 ng/L. This was not the case with a calculated concentration of 2,69 ng/L total PFOS. A possible reason for this is the drainage pipe that were near the sample location, which can have caused a lower concentration compared to sites close to the fire-fighting training sites.

The determined amount of total PFOS present in the sample from Ny-Ålesund was 273,82 ng/L. This was lower than the study the sample initially came from with a concentration of 310 ng/L. The lower amount of total PFOS is probably due to the measured values of L-PFOS and P6MHpS exceeding the linear range of the method and thus giving inaccurate concentrations. Based on the contribution of P6MHpS among the Br-PFOS isomers in T-PFOS and L-PFOS being the largest contributor. A larger range should be made to correctly quantitate samples with a general high level of PFOS.

6.Conclusion:

The current study tried to create a HPLC-MS/MS method using a fluorinated C18-PFP column for isomer specific determination of trace amounts of PFOS isomers in water samples. The separation of the target analytes resulted in 5 peaks whereas 3 of them consisted of separated peaks of P1MHpS, P6MHpS and L-PFOS. A better sensitivity was achieved due to the optimization of the MRM-transitions which resulted in a better response in comparison with the constant conditions of CE and fragmentation energies from the reference method.

The current method managed to achieve a better separation compared to the reference method using a C8 perfluorinated column. Based on the bandbroadening, peak shape, separation, general cost, and lifetime of the ACE Excel C18-PFP compared to the method using the perfluorinated C8 column the current method is more suitable for isomer specific target analysis of PFOS when using a HPLC-MS/MS setup.

The method for isomer specific determination was validated for all target analytes showing good linearity in the calibration standards and a precision within the validation criterion. A recovery range for the target analytes with the span 73% to 99% were satisfactory, but the calculated recovery for the Br-PFOS is uncertain due to the possibility of ISTD not being able to correct the loss of Br-PFOS during the sample preparation procedure properly. Another uncertainty was that not all isomers present in T-PFOS by ECF which likely contribute to worse accuracy and to higher calculated concentrations to some of the afflicted target analytes. The isomer profiles from each study site showed a larger contribution of branched PFOS than that present in T-PFOS, which fits the tendency of L-PFOS to sorb to soil and sediments.

The method lacked the necessary sensitivity to quantitate some of the target analytes in samples with a low level of PFOS due to their relatively low contribution in T-PFOS by ECF. Another sensitivity issue was the fact that the lower end of the calibration curve for the branched isomers were below the limit of quantification. The isomer profile from all study sites showed a higher contribution of Br-PFOS compared to its contribution in T-PFOS by ECF, which was the expected outcome. The sample from Sogna had a total amount of PFOS lower than expected in reference to earlier literature, but a possible cause was found. The sample from Fjellhamar river had expected levels of PFOS. The sample from Ny-Ålesund had uncertain values of L-PFOS and P6MHpS which is the probable reason for the lower measured concentration of total PFOS.

7.Future perspectives

Even though this analytical method was validated and managed to separate the PFOS isomers into 5 groups. This method has shown the possibilities of appliance of a C18-PFP column to separate PFOS isomers using a HPLC-MS/MS instrument. As this method used a guard column, an analysis without this column would provide insight on the separation managed by the ACE Excel C18-PFP column alone. Even though the method managed to get narrower peaks compared to the reference study, even narrower peaks could be achieved with the change of mobile phase composition or pH. Making calibration curves with a range reflecting on each isomer's contribution in T-PFOS would increase the possibilities of quantifying each target isomer. The method was not sensitive enough to detect the P35-/P45-/P55DMxS at low concentrations of PFOS. The sensitivity could be improved by reducing the band broadening of the peaks.

A more detailed method validation should also be done to assess the quality of the method. This should include a more elaborate test of robustness in the method, intermediate precision, checking the precision and accuracy at the lower end of the concentration. The use of spiked blank samples would differentiate between loss of analyte during sample preparation and matrix effects and would give a clearer view on the effects on using MPFOS as ISTD. The rigidity of the method could be tested by testing the method on different matrixes.

Another uncertainty of this method was the lack of standards that represent all PFOS isomers present in T-PFOS. If individual standards of these PFOS isomers were available on the market, it would be possible to identify possible coelution in environmental samples and would provide a more accurate isomer profile.

8.References

Abunada, Z., Alazaiza, M. Y. D. & Bashir, M. J. K. (2020). An Overview of Per- and Polyfluoroalkyl Substances (PFAS) in the Environment: Source, Fate, Risk and Regulations. *Water*, 12 (12): 3590.

Ahrens, L., Vogel, L. & Wiberg, K. (2018). Analysis of per-and polyfluoroalkyl substances (PFASs) and phenolic compounds in Swedish rivers over four different seasons.

Ali, A. M., Langberg, H. A., Hale, S. E., Kallenborn, R., Hartz, W. F., Mortensen, Å.-K., Ciesielski, T. M., McDonough, C. A., Jenssen, B. M. & Breedveld, G. D. (2021). The fate of poly- and perfluoroalkyl substances in a marine food web influenced by land-based sources in the Norwegian Arctic. *Environmental Science: Processes & Impacts*. doi: 10.1039/d0em00510j.

Arsenault, G., Chittim, B., Gu, J., McAlees, A., McCrindle, R. & Robertson, V. (2008). Separation and fluorine nuclear magnetic resonance spectroscopic (F-19 NMR) analysis of individual branched isomers present in technical perfluorooctanesulfonic acid (PFOS). *Chemosphere*, 73 (1): S53-S59. doi: 10.1016/j.chemosphere.2007.06.096.

Benskin, J. P., De Silva, A. O. & Martin, J. W. (2010). Isomer Profiling of Perfluorinated Substances as a Tool for Source Tracking: A Review of Early Findings and Future Applications. I: Whitacre, D. M. & DeVoogt, P. (red.) Reviews of Environmental Contamination and Toxicology, b. 208 *Reviews of Environmental Contamination and Toxicology, Vol 208: Perfluorinated Alkylated Substances*, s. 111-160.

Benskin, J. P., Muir, D. C. G., Scott, B. F., Spencer, C., De Silva, A. O., Kylin, H., Martin, J. W., Morris, A., Lohmann, R., Tomy, G., et al. (2012). Perfluoroalkyl Acids in the Atlantic and Canadian Arctic Oceans. *Environmental Science & Technology*, 46 (11): 5815-5823. doi: 10.1021/es300578x.

Beuthe, B., Dunk, M., Demeure, S., Carmona, J. M. M. & Medve, A. (2016). Environmental fate and effects of polyand perfluoroalkyl

substances (PFAS).

Braun, J. M. (2017). Early-life exposure to EDCs: role in childhood obesity and neurodevelopment. *Nature Reviews Endocrinology*, 13 (3): 161-173. doi: 10.1038/nrendo.2016.186.

Brennan, N. M., Evans, A. T., Fritz, M. K., Peak, S. A. & von Holst, H. E. (2021). Trends in the Regulation of Per- and Polyfluoroalkyl Substances (PFAS): A Scoping Review. *International Journal of Environmental Research and Public Health*, 18 (20). doi: 10.3390/ijerph182010900.

Buck, R. C., Franklin, J., Berger, U., Conder, J. M., Cousins, I. T., de Voogt, P., Jensen, A. A., Kannan, K., Mabury, S. A. & van Leeuwen, S. P. J. (2011). Perfluoroalkyl and polyfluoroalkyl substances in the environment: terminology, classification, and origins. *Integrated environmental assessment and management*, 7 (4): 513-41. doi: 10.1002/ieam.258.

Chen, C., Lu, Y., Zhang, X., Geng, J., Wang, T., Shi, Y., Hu, W. & Li, J. (2009). A review of spatial and temporal assessment of PFOS and PFOA contamination in China. *Chemistry and Ecology*, 25 (3): 163-177.

Chen, M., Wang, Q., Shan, G., Zhu, L., Yang, L. & Liu, M. (2018). Occurrence, partitioning and bioaccumulation of emerging and legacy per-and polyfluoroalkyl substances in Taihu Lake, China. *Science of the Total Environment*, 634: 251-259.

Company, M. (1997). Fluorochemical isomer distribution by 19F-NMR spectroscopy.
Conder, J. M., Hoke, R. A., De Wolf, W., Russell, M. H. & Buck, R. C. (2008). Are PFCAs bioaccumulative? A critical review and comparison with regulatory lipophilic compounds. *Environmental Science & Technology*, 42 (4): 995-1003. doi: 10.1021/es070895g.
Crinnion, W. J. (2010). The CDC Fourth National Report on Human Exposure to Environmental Chemicals: What it Tells Us About our Toxic Burden and How it Assists Environmental Medicine Physicians. *Alternative Medicine Review*, 15 (2): 101-108.
Forsvarsbygg. (2017). KJELLER BASE Innledende miljøkartlegging (Fase 1). doi: https://www.forsvarsbygg.no/globalassets/kjeller-base---innledende-miljokartlegging-fase-1.pdf.
Giesy, J. P. & Kannan, K. (2001). Global distribution of perfluorooctane sulfonate in wildlife. *Environmental Science & Technology*, 35 (7): 1339-1342. doi: 10.1021/es001834k.
Glenn, G., Shogren, R., Jin, X., Orts, W., Hart-Cooper, W. & Olson, L. (2021). Per- and polyfluoroalkyl substances and their alternatives in paper food packaging. *Comprehensive Reviews in Food Science and Food Safety*. doi: 10.1111/1541-4337.12726.
Higgins, C. P. & Luthy, R. G. (2006). Sorption of perfluorinated surfactants on sediments. *Environmental Science & Technology*, 40 (23): 7251-7256. doi: 10.1021/es061000n.
Houde, M., Martin, J. W., Letcher, R. J., Solomon, K. R. & Muir, D. C. G. (2006). Biological monitoring of polyfluoroalkyl substances: A review. *Environmental Science & Technology*, 40 (11): 3463-3473. doi: 10.1021/es052580b.
Houtz, E. F., Higgins, C. P., Field, J. A. & Sedlak, D. L. (2013). Persistence of Perfluoroalkyl Acid Precursors in AFFF-Impacted Groundwater and Soil. *Environmental Science & Technology*, 47 (15): 8187-8195. doi: 10.1021/es4018877.
ITRC. (2020). History and Use of Per- and Polyfluoroalkyl Substances (PFAS). *History and use*: 1-8.
Karrman, A., Langlois, I., van Bavel, B., Lindstrom, G. & Oehme, M. (2007). Identification and pattern of perfluorooctane sulfonate (PFOS) isomers in human serum and plasma. *Environment International*, 33 (6): 782-788. doi: 10.1016/j.envint.2007.02.015.
Kissa. (2001). Fluorinated Surfactants and Repellents, Second Edition Revised and Expanded. Andre utgave.
Kowalczyk, J., Flor, M., Karl, H. & Lahrssen-Wiederholt, M. (2020). Perfluoroalkyl substances (PFAS) in beaked redfish (Sebastes mentella) and cod (Gadus morhua) from arctic fishing grounds of Svalbard. *Food Additives & Contaminants Part B-Surveillance*, 13 (1): 34-44. doi: 10.1080/19393210.2019.1690052.
Lennikov, F. (2021). Distribution of perfluorooctanesulfunate (PFOS) isomers in a norwegian arctic food web.
OECD. (2002). Hazard assessment of perfluorooctane sulfonate (PFOS) and its salts. *ENV/JM/RD (2002) 17/FINAL*: 362.
OECD. (2018). Toward a New Comprehensive Global Database of Per- And Polyfluoroalkyl Substances (PFASs): Summary Report on Updating the OECD 2007 List of Per- and Polyfluoroalkyl Substances (PFASs). *Statistics*: 24.
Olsen, G. W., Church, T. R., Miller, J. P., Burris, J. M., Hansen, K. J., Lundberg, J. K., Armitage, J. B., Herron, R. M., Medhdizadehkashi, Z., Nobiletti, J. B., et al. (2003). Perfluorooctanesulfonate and other fluorochemicals in the serum of American Red

Cross adult blood donors. *Environmental Health Perspectives*, 111 (16): 1892-1901. doi: 10.1289/ehp.6316.

Olsen, G. W., Burris, J. M., Ehresman, D. J., Froehlich, J. W., Seacat, A. M., Butenhoff, J. L. & Zobel, L. R. (2007). Half-life of serum elimination of perfluorooctanesulfonate, perfluorohexanesulfonate, and perfluorooctanoate in retired fluorochemical production workers. *Environmental Health Perspectives*, 115 (9): 1298-1305. doi: 10.1289/ehp.10009.

Rayne, S. & Forest, K. (2009). Perfluoroalkyl sulfonic and carboxylic acids: A critical review of physicochemical properties, levels and patterns in waters and wastewaters, and treatment methods. *Journal of Environmental Science and Health Part a-Toxic/Hazardous Substances & Environmental Engineering*, 44 (12): 1145-1199. doi: 10.1080/10934520903139811.

Saikat, S., Kreis, I., Davies, B., Bridgman, S. & Kamanyire, R. (2013). The impact of PFOS on health in the general population: a review. *Environmental Science: Processes & Impacts*, 15 (2): 329-335.

Schulz, K., Silva, M. R. & Klaper, R. (2020). Distribution and effects of branched versus linear isomers of PFOA, PFOS, and PFHxS: A review of recent literature. *Science of the Total Environment*, 733. doi: 10.1016/j.scitotenv.2020.139186.

Skaar, J. S., Ræder, E. M., Lyche, J. L., Ahrens, L. & Kallenborn, R. (2019). Elucidation of contamination sources for poly-and perfluoroalkyl substances (PFASs) on Svalbard (Norwegian Arctic). *Environmental Science and Pollution Research*, 26 (8): 7356-7363.

Sunderland, E. M., Hu, X. D. C., Dassuncao, C., Tokranov, A. K., Wagner, C. C. & Allen, J. G. (2019). A review of the pathways of human exposure to poly- and perfluoroalkyl substances (PFASs) and present understanding of health effects. *Journal of Exposure Science and Environmental Epidemiology*, 29 (2): 131-147. doi: 10.1038/s41370-018-0094-1.

USEPA. (2018). Long-Chain Perfluoroalkyl Carboxylate and Perfluoroalkyl Sulfonate Chemical Substances; Significant New Use Rule.

Wang, T., Wang, Y. W., Liao, C. Y., Cai, Y. Q. & Jiang, G. B. (2009). Perspectives on the Inclusion of Perfluorooctane Sulfonate into the Stockholm Convention on Persistent Organic Pollutants. *Environmental Science & Technology*, 43 (14): 5171-5175. doi: 10.1021/es900464a.

Yamashita, N., Kannan, K., Taniyasu, S., Horii, Y., Petrick, G. & Gamo, T. (2005). A global survey of perfluorinated acids in oceans. *Marine Pollution Bulletin*, 51 (8-12): 658-668. doi: 10.1016/j.marpolbul.2005.04.026.

Appendix

Appendix A: Contribution of PFOS isomers in PFOS

Table A-1: Contribution of PFOS isomers present in T-PFOS according to a study by Arsenault et. al. 2008.	
LPFOS	62,3
P1MHpS	2,4
P2MHpS	2,2
P3MHpS	6,5
P4MHpS	5,3
P5MHpS	8,0
P6MHpS	11,4
P35DMHxS	0,12
P45DMHxS	0.13
P55DMHxS	0.56

Appendix B: Standards, reagents, materials and instruments

Table B-1: Complete list of chemicals					
Full name	CAS-number	Supplier	Purity	Size	Use
Ammonium acetate	631-61-8	VWR International AS	>99%	500 g	Buffersolution for mobile phase A and B
Ammonium hydroxide	1336-21-6	Merck, Germany	25%	500 mL	Solvent during extraction
Sodium acetate	127-09-3	Sigma-Aldrich, USA	>99%	500 g	Buffersolution for extractions
Acetic acid	64-19-7	Sigma-Aldrich, USA	>99%	500 mL	Buffer solution for extractions
Methanol	67-56-1	VWR International AS	>99%	2,5 L	Mobile phase, solvent and cleanup during extraction

Table B-2: complete list of standards				
Name	acronym	CAS number	Supplier	Purity
Sodium perfluoro-1-[1,2,3,4-13C4] octanesulfonate	MPFOS	960315-53-1	Wellington Laboratories, Guelph, ON, Canada	>99%
Sodium perfluoro-1-octanesulfonate	L-PFOS	4021-47-0	Wellington Laboratories, Guelph, ON, Canada	>99%
Perfluoro-1-methylheptane sulfonate	P1MHpS	Not available	Wellington Laboratories, Guelph, ON, Canada	>99%
Perfluoro-3-methylheptane sulfonate	P3MHpS	Not available	Wellington Laboratories, Guelph, ON, Canada	>99%
Perfluoro-4-methylheptane sulfonate	P4MHpS	Not available	Wellington Laboratories, Guelph, ON, Canada	>99%
Perfluoro-5-methylheptane sulfonate	P5MHpS	Not available	Wellington Laboratories, Guelph, ON, Canada	>99%
Perfluoro-6-methylheptane sulfonate	P6MHpS	Not available	Wellington Laboratories, Guelph, ON, Canada	>99%
Perfluoro-3,5-dimethylhexane sulfonic acid	P35DMHxS	Not available	Wellington Laboratories, Guelph, ON, Canada	>99%
Perfluoro-4,5-dimethylhexane sulfonic acid	P45DMHxS	Not available	Wellington Laboratories, Guelph, ON, Canada	>99%
Perfluoro-5,5-dimethylhexane sulfonic acid	P55DMHxS	Not available	Wellington Laboratories, Guelph, ON, Canada	>99%

Table B-3	
Name	Supplier
Proline Automatic pipette 5-50 µL	Biohit, Helsinki Finland
Proline Automatic pipette 10-100 µL	Biohit, Helsinki Finland
Proline Automatic pipette 100-1000 µL	Biohit, Helsinki Finland
Pipette tips 200µL	Brand, Wertheim Germany
Pipette tips 1000 µL	Brand, Wertheim Germany
Pasteur Pipettes	VWR International AS
Oasis WAX 6cc 500 mg	Waters, USA
Nitrile purple gloves	VWR International AS
Spin-X centrifuge tube filters	Costar, Corning, NY, USA

Table B-4: Complete list of instruments		
Name	Producer	Description
6400 Series Triple Quadrupole LC/MS	Agilent Technologies, Santa Clara, CA, USA	
Agilent 1200 Series HPLC system	Agilent Technologies, Santa Clara, CA, USA	
Agilent 1200 Series High Performance Autosampler	Agilent Technologies, Santa Clara, CA, USA	
Agilent 1200 Series Binary Pump	Agilent Technologies, Santa Clara, CA, USA	
Agilent 1200 Series Column Compartment	Agilent Technologies, Santa Clara, CA, USA	
Masshunter Workstation software: Quantitative analysis for QQQ	Agilent Technologies, Santa Clara, CA, USA	SW version B.10.01
MassHunter Workstation Software: Qualitative analysis for QQQ version B.06.00 / Build 6.0.633.10	Agilent Technologies, Santa Clara, CA, USA	SW version B.10.01
Vacuum Manifold	Agilent Technologies, Santa Clara, CA, USA	

Table B-4: Complete list of instruments		
ACE Excel 3 C18-PFP (100 Å, 100x2.1 mm id, 3 um)	Advanced Chromatography Technologies (ACE), United Kingdom	
Eclipse Plus C18 (2.1x5mm id, 1,8um)	Agilent Technologies, Santa Clara, CA, USA	Guard column
Vortex mixer	VWR International AS, Oslo, Norway	

Appendix C: Flowchart of the method

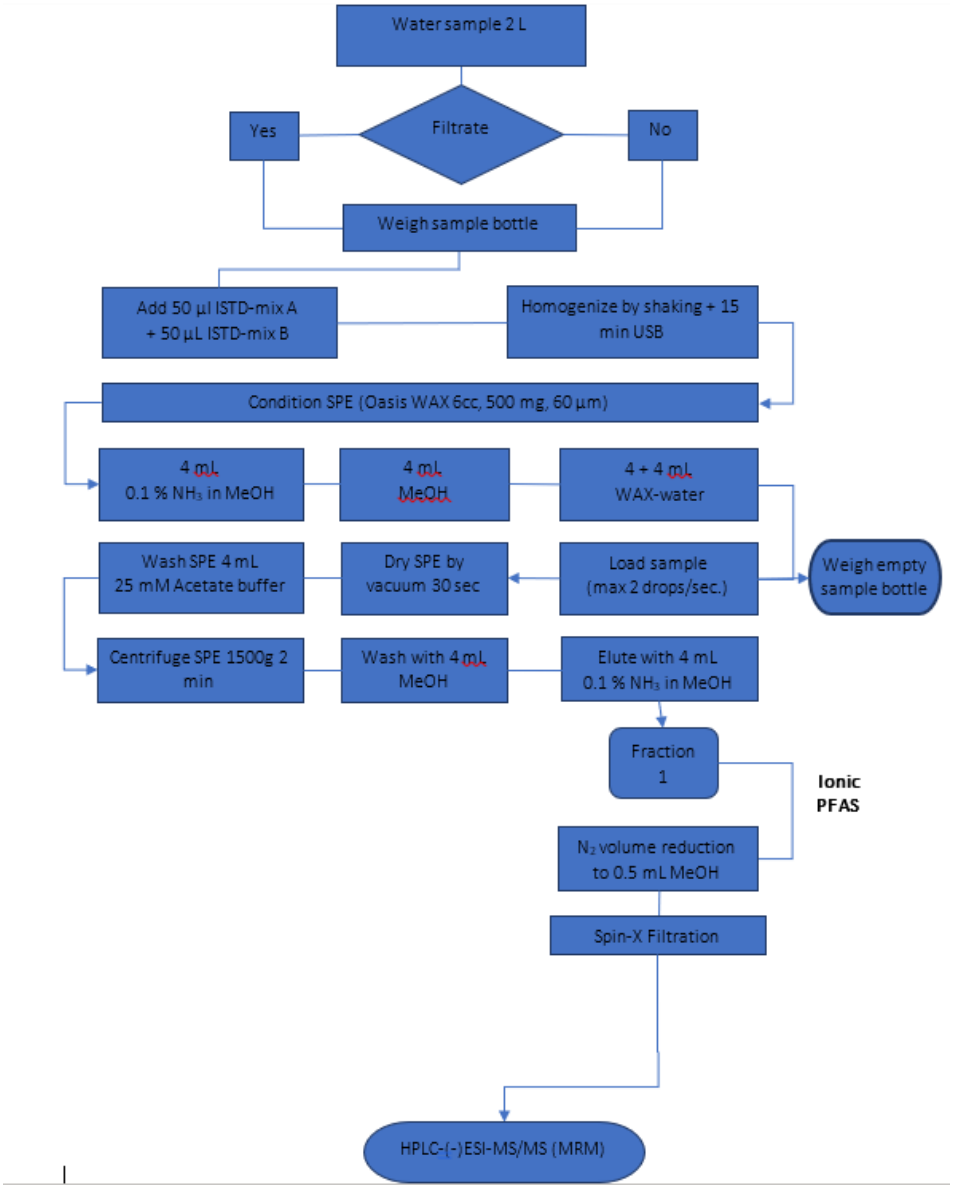

Figure C-1 Flowchart of the sample preparation procedure. The procedure has been used in multiple studies including the study where the sample from Ny-Ålesund have been analyzed (Skaar et al., 2019)

Appendix D: MS-parameters

D-1 MS-parameters with the decided and optimized MRM-transitions in the study.

Method Name	Br-PFOS metode test brattere gradient 1.m
Method Path	D:\MassHunter\Methods\Mathias\C18 metode utvikling\Br-PFOS metode test brattere gradient 1.m
Method Description	6460 Triple Quad LC/MS ESI with Agilent Jet Stream Technology Positive MS2 Background Scan Method

Device List

HiP Sampler
Binary Pump
Column Comp.
QQQ

Ion Source	AJS ESI	**Tune File**	D:\MassHunter\Tune\QQQ\G6460A \atunes.TUNE.XML
Stop Mode	No Limit/As Pump	**Stop Time (min)**	No limit
Time Filter	Off	**Time Filter Width (min)**	0.07

Time Segments

Index	Start Time (min)	Scan Type	Ion Mode	Div Valve	Delta EMV (-)	Store
1	0	MRM	ESI+Agilent Jet Stream	To MS	400	Yes

Time Segment 1

Scan Segments

Cpd Group	Cpd Name	ISTD?	Prec Ion	MS1 Res	Prod Ion	MS2 Res	Dwell	Frag (V)	CE (V)	Cell Acc (V)	Polarity
M4PFOS	MPFOS	No	503	Unit/Enh (6490)	99	Unit/Enh (6490)	30	200	76	6	Negative
M4PFOS	MPFOS	No	503	Unit/Enh (6490)	80	Unit/Enh (6490)	30	200	76	6	Negative
PFOS	P1MHpS	No	499	Unit/Enh (6490)	419	Unit/Enh (6490)	30	125	25	6	Negative
PFOS	P45DMHpS	No	499	Unit/Enh (6490)	330	Unit/Enh (6490)	30	140	32	6	Negative
PFOS	P3MHpS	No	499	Unit/Enh (6490)	280	Unit/Enh (6490)	30	150	35	6	Negative
PFOS	P5MHpS	No	499	Unit/Enh (6490)	230	Unit/Enh (6490)	30	200	41	6	Negative
PFOS	P4MHpS	No	499	Unit/Enh (6490)	230	Unit/Enh (6490)	30	220	37	6	Negative
PFOS	P6MHpS	No	499	Unit/Enh (6490)	230	Unit/Enh (6490)	30	150	55	6	Negative
PFOS	P55DMHpS	No	499	Unit/Enh (6490)	219	Unit/Enh (6490)	30	230	42	6	Negative
PFOS	P5MHpS	No	499	Unit/Enh (6490)	130	Unit/Enh (6490)	30	160	46	6	Negative
PFOS	P45DMHpS	No	499	Unit/Enh (6490)	130	Unit/Enh (6490)	30	150	46	6	Negative
PFOS	P1MHpS	No	499	Unit/Enh (6490)	99	Unit/Enh (6490)	30	160	37	6	Negative
PFOS	LPFOS	No	499	Unit/Enh (6490)	99	Unit/Enh (6490)	30	170	35	6	Negative
PFOS	P6MHpS	No	499	Unit/Enh (6490)	80	Unit/Enh (6490)	30	190	45	6	Negative
PFOS	P55DMHpS	No	499	Unit/Enh (6490)	80	Unit/Enh (6490)	30	210	63	6	Negative
PFOS	P4MHpS	No	499	Unit/Enh (6490)	80	Unit/Enh (6490)	30	210	63	6	Negative
PFOS	P3MHpS	No	499	Unit/Enh (6490)	80	Unit/Enh (6490)	30	200	66	6	Negative
PFOS	LPFOS	No	499	Unit/Enh (6490)	80	Unit/Enh (6490)	30	210	67	6	Negative

Scan Parameters

Data Stg	Threshold
Centroid	0

Source Parameters

Parameter	Value (+)	Value (-)
Gas Temp (°C)	300	300
Gas Flow (l/min)	5	5
Nebulizer (psi)	25	25
Sheath Gas Temp (°C)	350	350
Sheath Gas Flow (l/min)	11	11
Capillary (V)	2000	2500
Nozzle Voltage/Charging (V)	2000	500

Chromatograms

Chrom Type	Label	Offset	Y-Range
TIC	TIC	0	10000000

Instrument Curves

Actual

Name: HiP Sampler **Model:** G1367C

Auxiliary	
Draw Speed	200.0 µL/min
Eject Speed	200.0 µL/min
Draw Position Offset	0.0 mm
Wait Time After Drawing	0.0 s
Sample Flush Out Factor	5.0
Vial/Well bottom sensing	No
Injection	
Injection Mode	Injection with needle wash
Injection Volume	5.00 µL
Needle Wash	
Needle Wash Location	Flush Port
Wash Time	5.0 s
High throughput	
Automatic Delay Volume Reduction	No
Overlapped Injection	
Enable Overlapped Injection	No
Valve Switching	
Valve Movements	1
Valve Switch Time 1	
Switch Time 1 Enabled	No
Valve Switch Time 2	
Switch Time 2 Enabled	No
Valve Switch Time 3	
Switch Time 3 Enabled	No
Valve Switch Time 4	
Switch Time 4 Enabled	No
Stoptime	
Stoptime Mode	As Pump/No Limit
Posttime	
Posttime Mode	Off

Name: Binary Pump **Model:** G1312B

Flow	0.400 mL/min
Use Solvent Types	Yes
Low Pressure Limit	0.00 bar
High Pressure Limit	600.00 bar
Maximum Flow Gradient	100.000 mL/min²
Stroke A	
Automatic Stroke Calculation A	Yes
Stroke B	
Automatic Stroke Calculation B	Yes
Stoptime	
Stoptime Mode	Time set
Stoptime	25.00 min
Posttime	
Posttime Mode	Off

Solvent Composition

	Channel	Solvent 1	Name 1	Solvent 2	Name 2	Selected	Used	Percent
1	A	H20	10% MeOH+ NH4 Form.	H20	A2	Ch. 1	Yes	50.0 %
2	B	MeOH	MeOH	MeOH	MeOH	Ch. 1	Yes	50.0 %

Timetable

	Time	A	B	Flow	Pressure
1	8.00 min	50.0 %	50.0 %	--- mL/min	--- bar
2	15.00 min	15.0 %	85.0 %	--- mL/min	--- bar
3	17.00 min	0.0 %	100.0 %	--- mL/min	--- bar
4	19.00 min	50.0 %	50.0 %	--- mL/min	--- bar
5	25.00 min	50.0 %	50.0 %	--- mL/min	--- bar

Name: Column Comp. **Model:** G1316B

Valve Position	Position 1 (Port 1 -> 2)
Left Temperature Control	
Temperature Control Mode	Temperature Set
Temperature	40.0 °C
Enable Analysis Left Temperature	
Enable Analysis Left Temperature On	Yes
Enable Analysis Left Temperature Value	0.8 °C
Right Temperature Control	
Right temperature Control Mode	Temperature Set
Right temperature	40.0 °C
Enable Analysis Right Temperature	
Enable Analysis Right Temperature On	Yes
Enable Analysis Right Temperature Value	0.8 °C
Stoptime	
Stoptime Mode	As Pump/Injector
Posttime	
Posttime Mode	Off
Timetable	

D-2: MRM transitions from the reference study.

Scan Segments

Cpd Group	Cpd Name	ISTD?	Prec Ion	MS1 Res	Prod Ion	MS2 Res	Dwell	Frag (V)	CE (V)	Cell Acc (V)	Polarity
	MPFOS	Yes	503	Unit/Enh (6490)	99	Unit/Enh (6490)	30	200	61	6	Negative
	MPFOS	Yes	503	Unit/Enh (6490)	80	Unit/Enh (6490)	30	200	61	6	Negative
	PFOS	No	499	Unit/Enh (6490)	419	Unit/Enh (6490)	30	200	61	6	Negative
	P45DMHxS	No	499	Unit/Enh (6490)	330	Unit/Enh (6490)	30	200	61	6	Negative
	P44DMHxS	No	499	Unit/Enh (6490)	330	Unit/Enh (6490)	30	200	61	6	Negative
	PFOS	No	499	Unit/Enh (6490)	330	Unit/Enh (6490)	30	200	61	6	Negative
	P55DMHxS	No	499	Unit/Enh (6490)	320	Unit/Enh (6490)	30	200	61	6	Negative
	P45DMHxS	No	499	Unit/Enh (6490)	230	Unit/Enh (6490)	30	200	61	6	Negative
	P44DMHxS	No	499	Unit/Enh (6490)	230	Unit/Enh (6490)	30	200	61	6	Negative
	P6MHpS	No	499	Unit/Enh (6490)	230	Unit/Enh (6490)	30	200	61	6	Negative
	PFOS	No	499	Unit/Enh (6490)	230	Unit/Enh (6490)	30	200	61	6	Negative
	P55DMHxS	No	499	Unit/Enh (6490)	219	Unit/Enh (6490)	30	200	61	6	Negative
	P5MHpS	No	499	Unit/Enh (6490)	219	Unit/Enh (6490)	30	200	61	6	Negative
	P1MHpS	No	499	Unit/Enh (6490)	219	Unit/Enh (6490)	30	200	61	6	Negative
	PFOS	No	499	Unit/Enh (6490)	219	Unit/Enh (6490)	30	200	61	6	Negative
	P6MHpS	No	499	Unit/Enh (6490)	169	Unit/Enh (6490)	30	200	61	6	Negative
	P1MHpS	No	499	Unit/Enh (6490)	169	Unit/Enh (6490)	30	200	61	6	Negative
	L-PFOS	No	499	Unit/Enh (6490)	169	Unit/Enh (6490)	30	200	61	6	Negative
	PFOS	No	499	Unit/Enh (6490)	169	Unit/Enh (6490)	30	200	61	6	Negative
	P45DMHxS	No	499	Unit/Enh (6490)	130	Unit/Enh (6490)	30	200	61	6	Negative
	P44DMHxS	No	499	Unit/Enh (6490)	130	Unit/Enh (6490)	30	200	61	6	Negative
	P5MHpS	No	499	Unit/Enh (6490)	130	Unit/Enh (6490)	30	200	61	6	Negative
	P3MHpS	No	499	Unit/Enh (6490)	130	Unit/Enh (6490)	30	200	61	6	Negative
	PFOS	No	499	Unit/Enh (6490)	130	Unit/Enh (6490)	30	200	61	6	Negative
	PFOS	No	499	Unit/Enh (6490)	119	Unit/Enh (6490)	30	200	61	6	Negative
	P6MHpS	No	499	Unit/Enh (6490)	99	Unit/Enh (6490)	30	200	61	6	Negative
	P3MHpS	No	499	Unit/Enh (6490)	99	Unit/Enh (6490)	30	200	61	6	Negative
	P1MHpS	No	499	Unit/Enh (6490)	99	Unit/Enh (6490)	30	200	61	6	Negative
	L-PFOS	No	499	Unit/Enh (6490)	99	Unit/Enh (6490)	30	200	61	6	Negative
	PFOS	No	499	Unit/Enh (6490)	99	Unit/Enh (6490)	30	200	61	6	Negative
	P55DMHxS	No	499	Unit/Enh (6490)	80	Unit/Enh (6490)	30	200	61	6	Negative
	P45DMHxS	No	499	Unit/Enh (6490)	80	Unit/Enh (6490)	30	200	61	6	Negative
	P44DMHxS	No	499	Unit/Enh (6490)	80	Unit/Enh (6490)	30	200	61	6	Negative
	P6MHpS	No	499	Unit/Enh (6490)	80	Unit/Enh (6490)	30	200	61	6	Negative
	P5MHpS	No	499	Unit/Enh (6490)	80	Unit/Enh (6490)	30	200	61	6	Negative
	P3MHpS	No	499	Unit/Enh (6490)	80	Unit/Enh (6490)	30	200	61	6	Negative
	L-PFOS	No	499	Unit/Enh (6490)	80	Unit/Enh (6490)	30	200	61	6	Negative
	PFOS	No	499	Unit/Enh (6490)	80	Unit/Enh (6490)	30	200	61	6	Negative
	PFOS	No	499	Unit/Enh (6490)	58	Unit/Enh (6490)	30	200	61	6	Negative
	PFOA	No	413	Unit/Enh (6490)	369	Unit/Enh (6490)	30	76	45	6	Negative
	PFOA	No	413	Unit/Enh (6490)	219	Unit/Enh (6490)	30	200	61	6	Negative
	PFOA	No	413	Unit/Enh (6490)	169	Unit/Enh (6490)	30	76	45	6	Negative
	PFOA	No	413	Unit/Enh (6490)	119	Unit/Enh (6490)	30	200	61	6	Negative

Table D-2: Mobile phase composition and gradient program in the reference method.

Solvent Composition

	Channel	Solvent 1	Name 1	Solvent 2	Name 2	Selected	Used	Percent
1	A	H20	10 mM NH4 Form.	H20	A2	Ch. 1	Yes	65.0 %
2	B	MeOH	MeOH	MeOH	MeOH	Ch. 1	Yes	35.0 %

Timetable

	Time	A	B	Flow	Pressure
1	0.30 min	65.0 %	35.0 %	0.150 mL/min	600.00 bar
2	1.90 min	36.0 %	64.0 %	0.150 mL/min	600.00 bar
3	5.90 min	34.0 %	66.0 %	0.150 mL/min	600.00 bar
4	7.90 min	30.0 %	70.0 %	0.150 mL/min	600.00 bar
5	28.00 min	25.0 %	75.0 %	0.150 mL/min	600.00 bar
6	29.00 min	0.0 %	100.0 %	0.150 mL/min	600.00 bar
7	35.00 min	65.0 %	35.0 %	0.150 mL/min	600.00 bar
8	45.00 min	65.0 %	35.0 %	0.150 mL/min	600.00 bar

Appendix E: Chromatograms

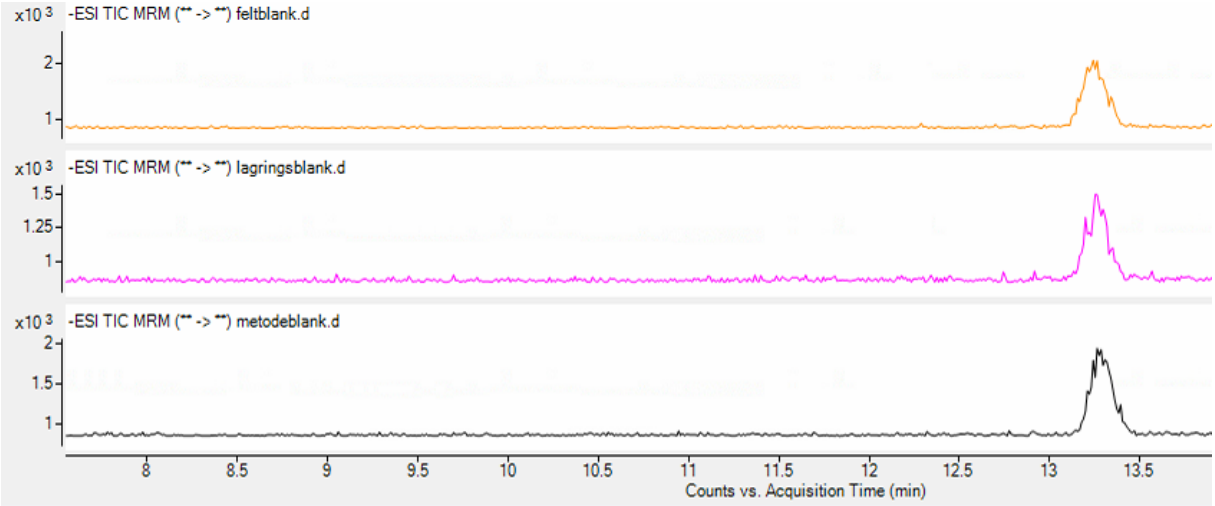

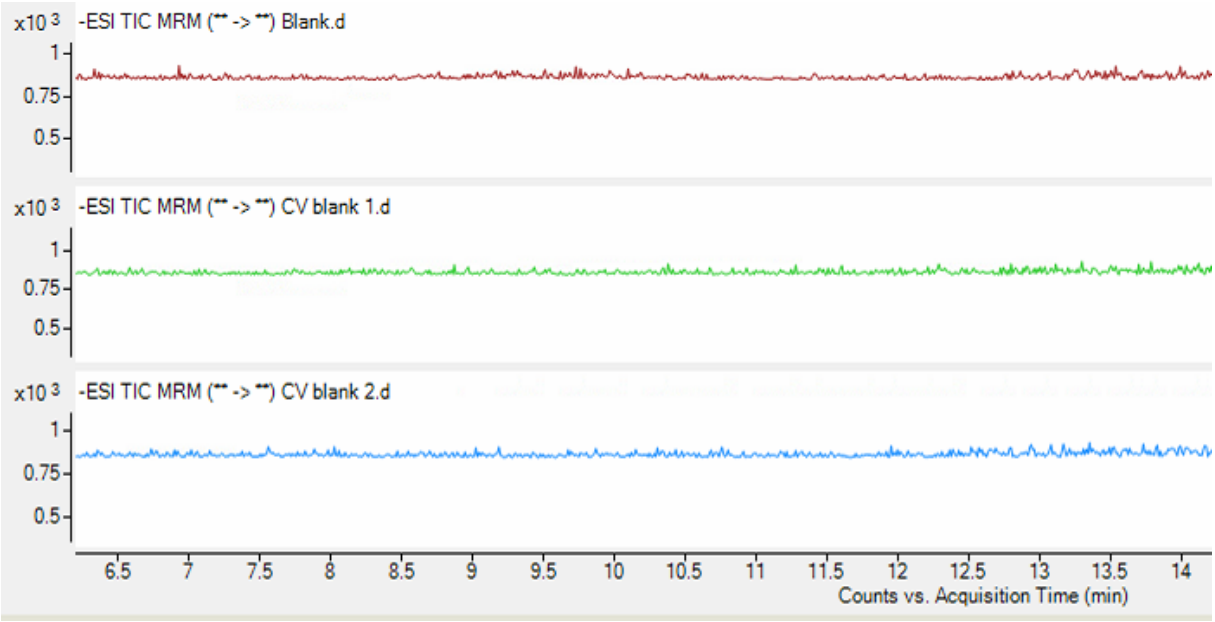

Figure E-1: Excamples of procedural blanks (1) and (2) instrument blanks achieved by the analytical method.

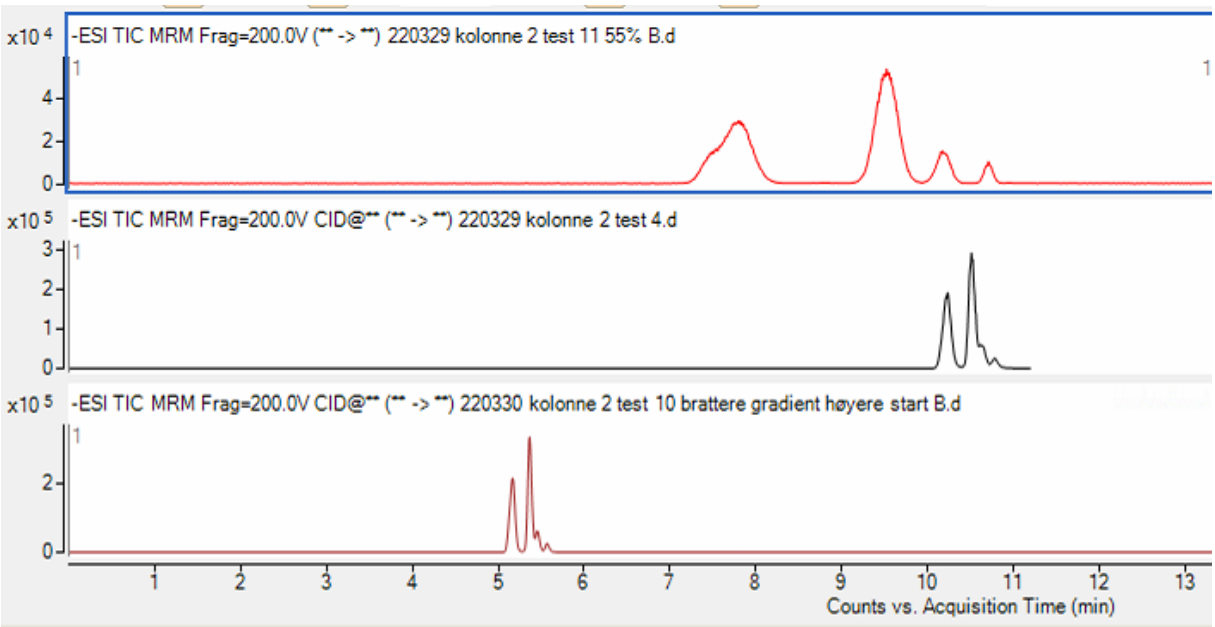

Figure E-2: Chromatograms showing separation during the analythical method development

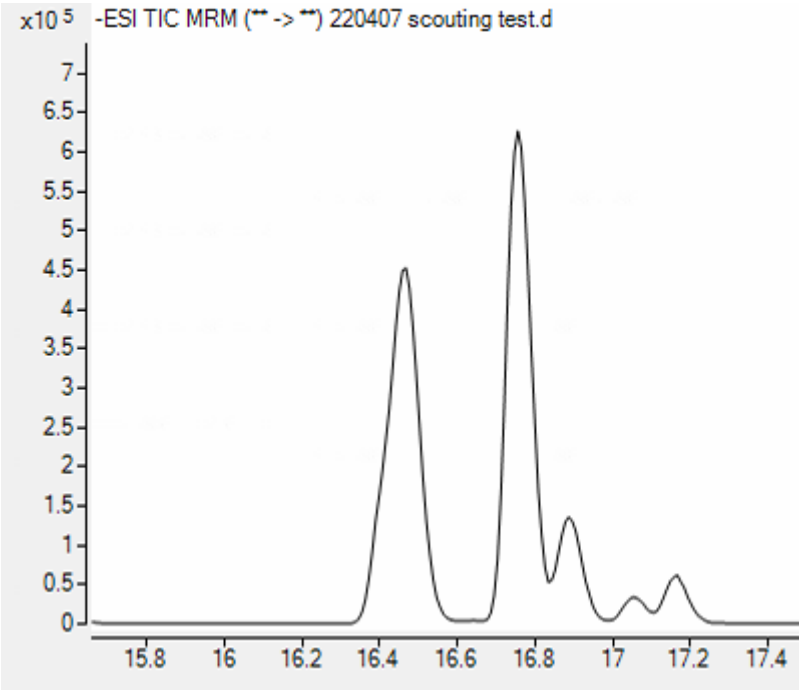

Figure E-3: Chromatogram of the scouting gradient with a mix of all the target isomers.

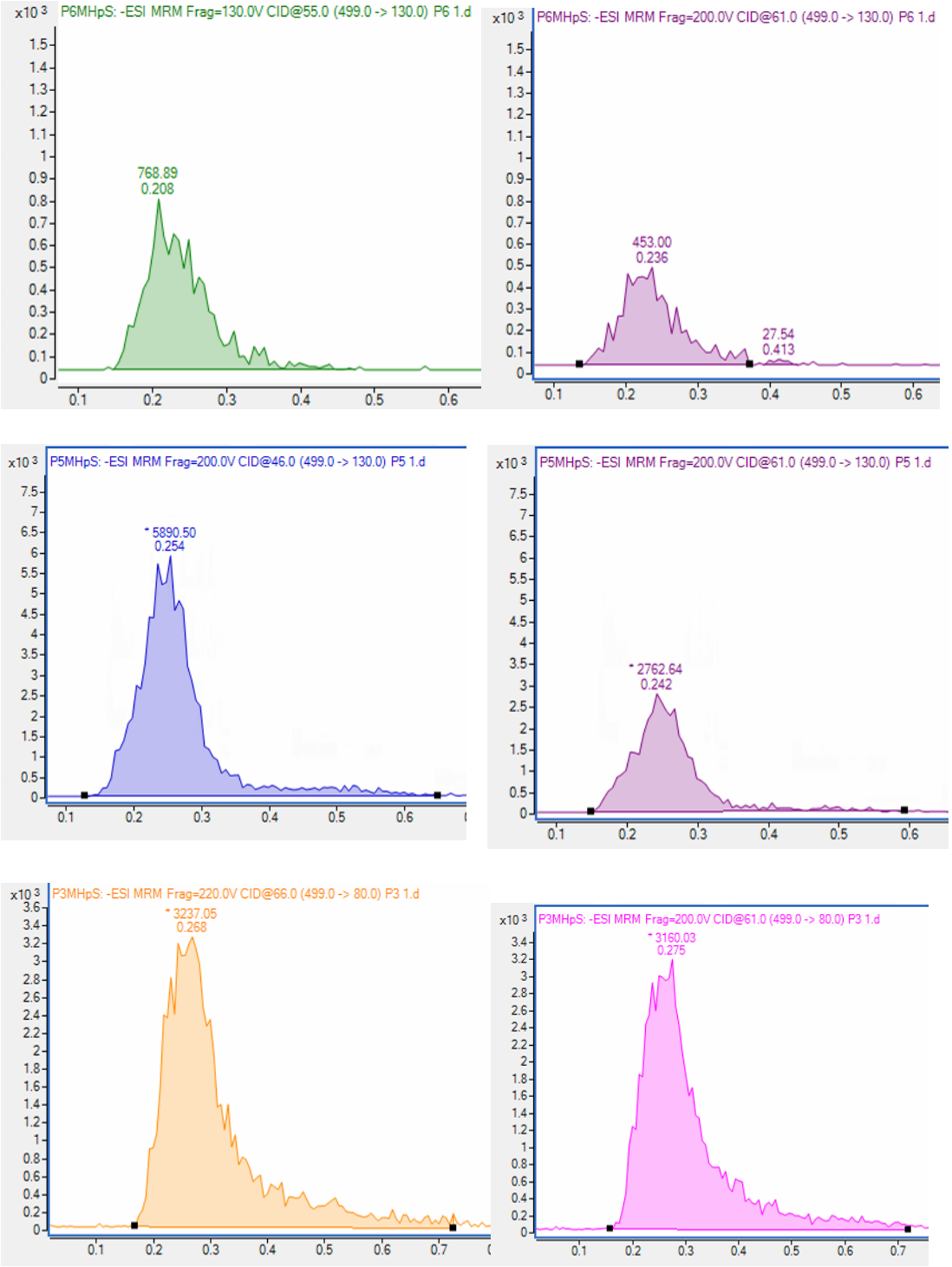

Figure E-4 Examples of improved response (left) compared to the constant fragmentation energy (200V) and CE (61 eV) used in the reference method (right). The chromatograms are a result of direct injection of each standard.

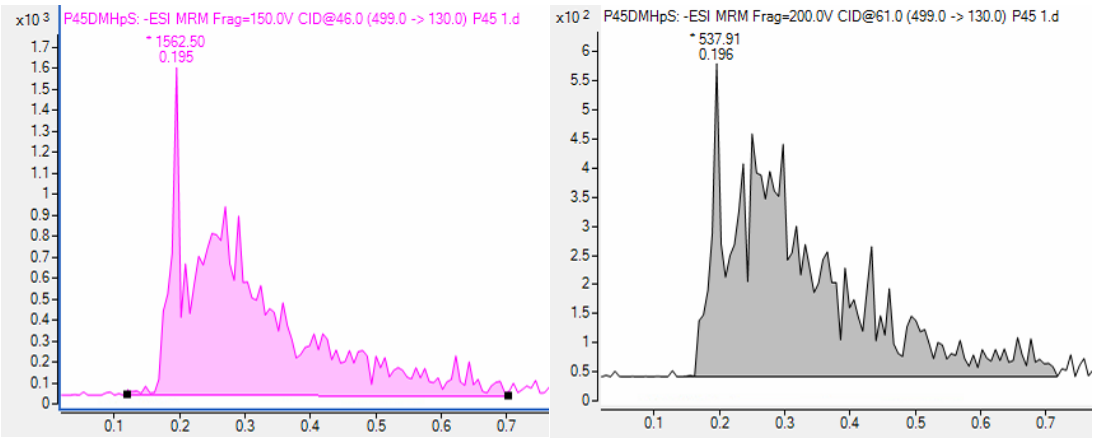

Figure E-4 Examples of improved response (left) compared to the constant fragmentation energy (200V) and CE (61 eV) used in the reference method (right). The chromatograms are a result of direct injection of each standard.

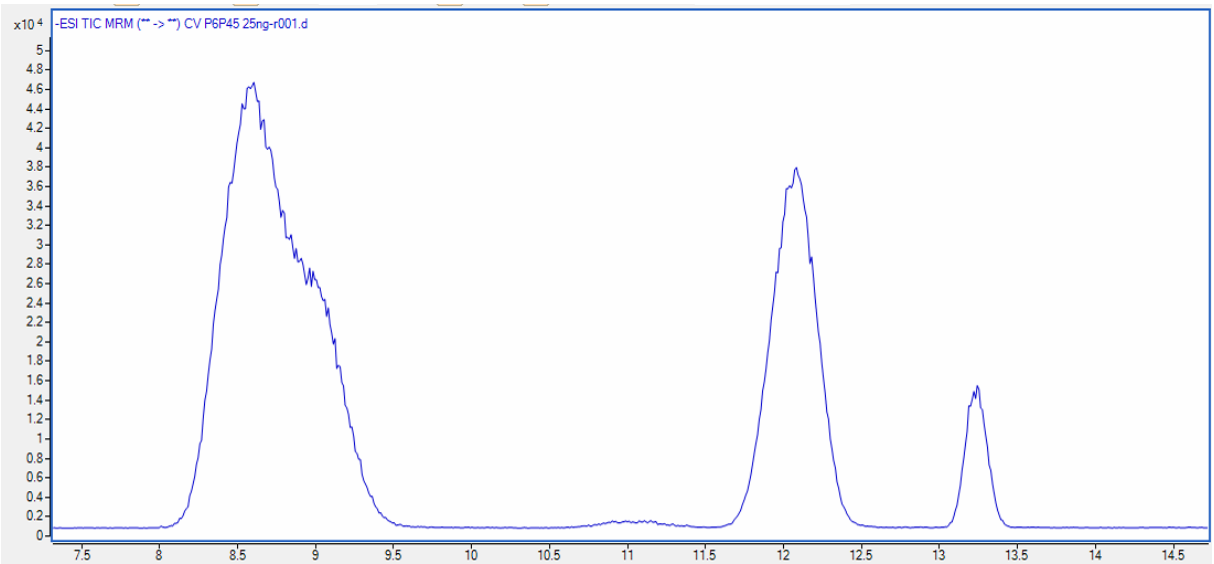

Figure E-5: Chromathogram of P35-/P45DMHxS (left), P6MHpS (middle) and ISTD response (right).

(1) (2)

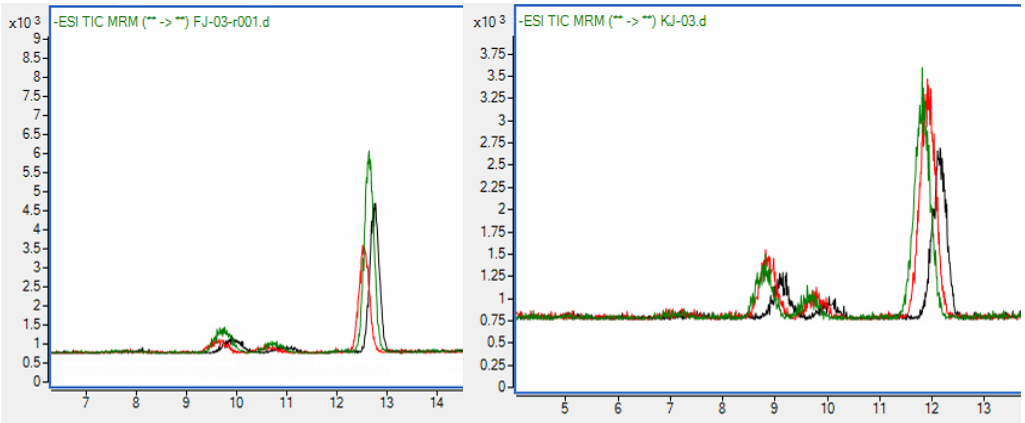

(3)

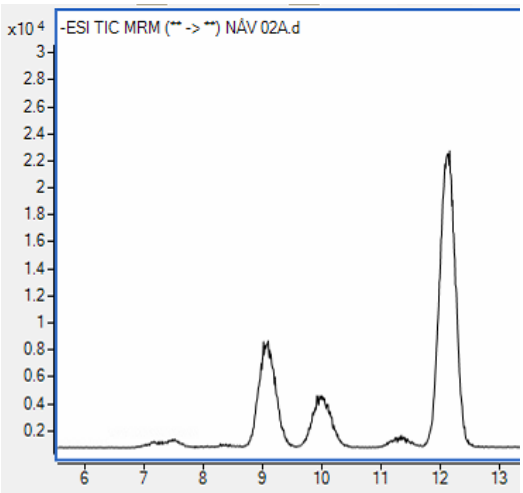

Figure E-6: Chromatograms of the sample(s) from Fjellhamardammen environmental park (1), Sogna (2) and Ny-Ålesund (3)

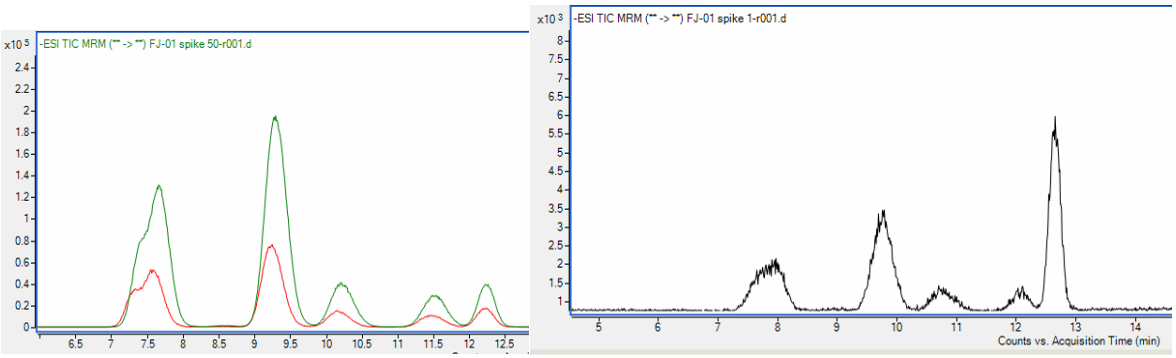

Figure E-6: chromatograms of the spiked samples of 50 ng/mL (green), 25 ng/mL (red) and 1 ng/mL (left)

Appendix F: calibration curves of the analytes and individual isomers

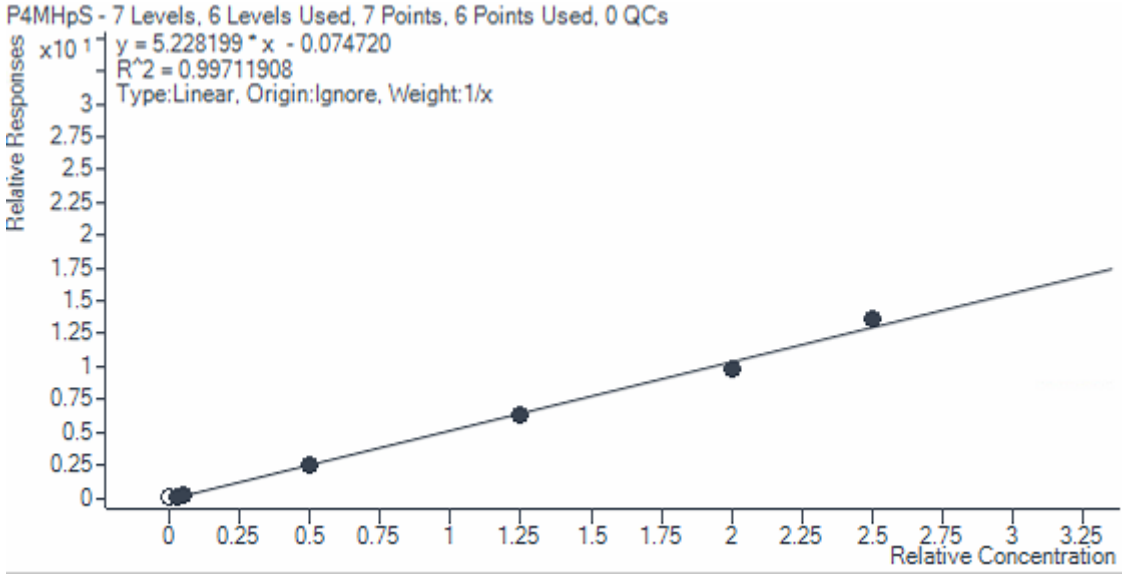

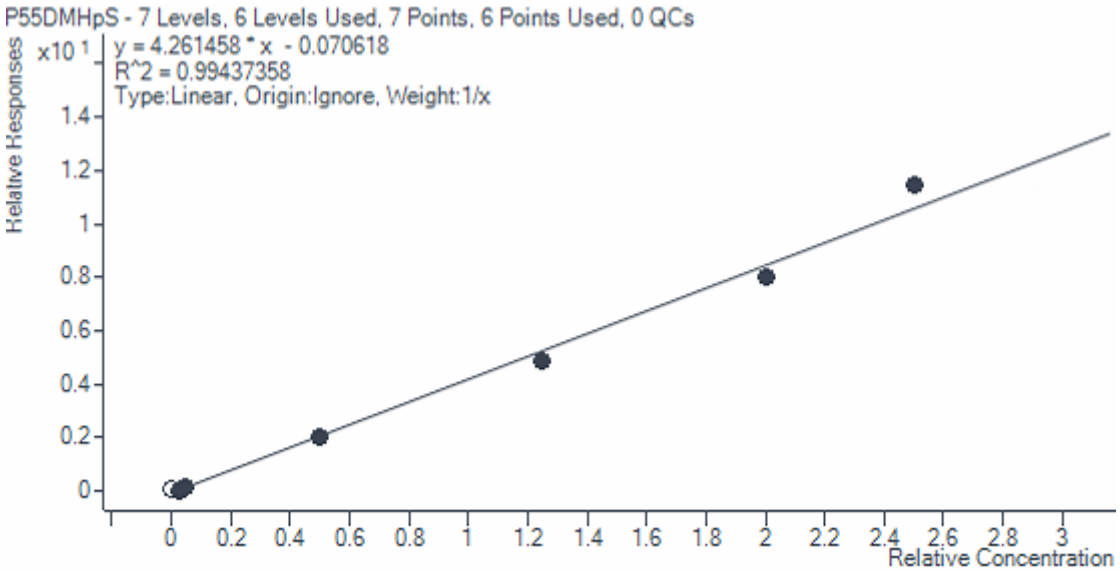

Figure F-1 Calibration curves of the coeluting isomers used to quantitate coelution.

Calibration curves of the separated target isomers:

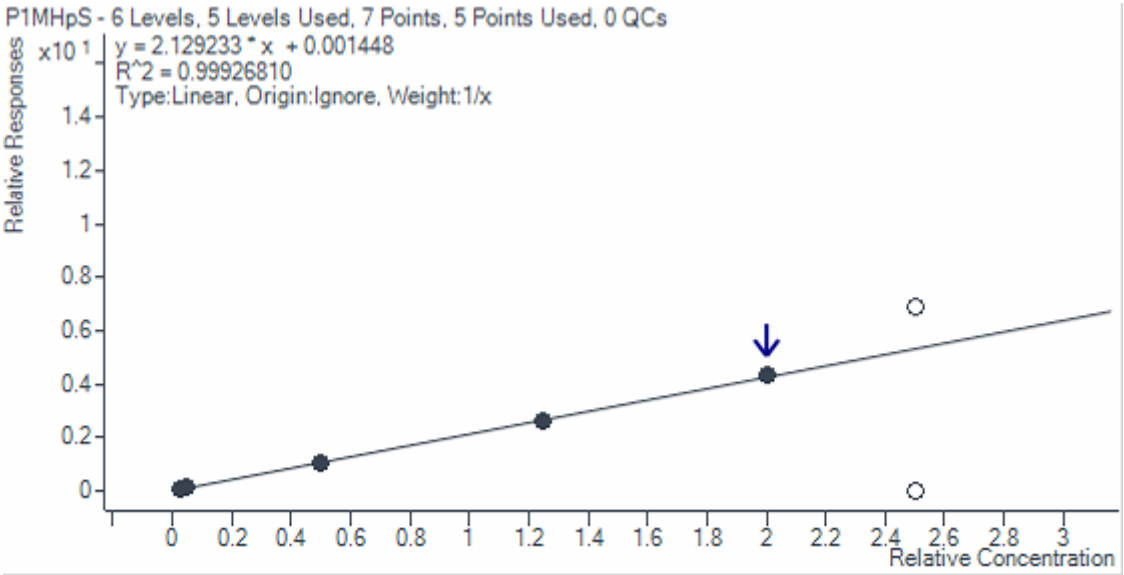

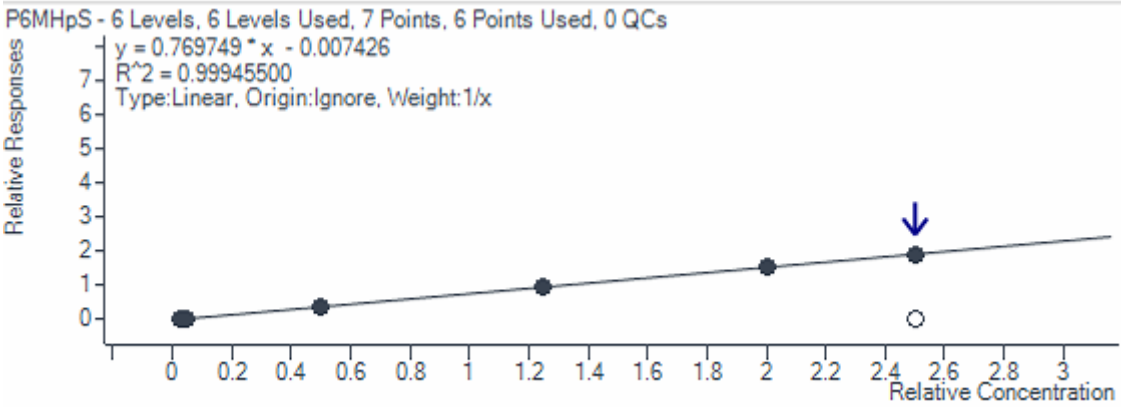

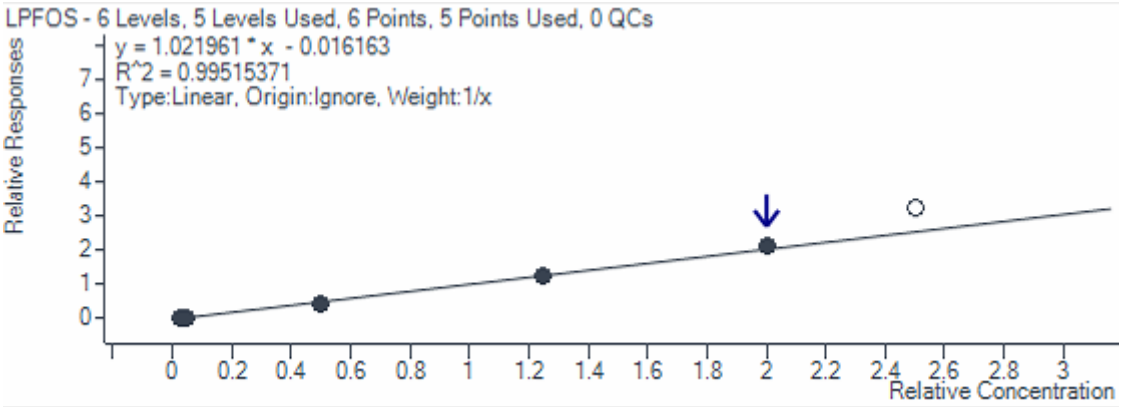

Appendix G: Raw data

Table G-1: Rawdata from (A) L-PFOS, (B) P1MHpS, (C) P6MHpS, (D) coeluted P3-P4-P5MHpS and (E) P35-/P45-/P55DMHxS. The samples marked in blue was left out from the calibration curve. Concentrations above the LOQ is marked with turquoise while concentrations below LOQ is marked with red for the relevant samples. Note that some of these samples was not included in this thesis. The sample from Ny-Ålesund is marked with bold characters as **NÅV 02 A 10X**.

A

	LPFOS Results				MPFOS (ISTD) Results	
Name	Area	RT	Calc. Conc.	Area	RT	Resp.
L-PFOS STD 50	152891	13,35	63,54	45164	13,318	47326
L-PFOS STD 40	105908	13,36	41,83	33517	13,34	49929
L-PFOS STD 25	66791,5	13,35	24,65	20519	13,351	53724
L-PFOS STD 10	23683,7	13,29	8,49	7586,6	13,318	56681
L-PFOS STD 1	1926,35	13,41	0,94	681,54	13,373	60097
L-PFOS STD 0,5	828,61	13,36	0,59	273,32	13,373	59747
FJ-01	2202,97	13,25	2,49	680	13,253	19873
FJ-02	2195,66	13,23	2,61	710,85	13,221	18717
FJ-03	4022,83	13,23	2,53	1165,2	13,232	35611
FJ-03 Spike 1 ng	4237,29	13,22	3,21	1508,3	13,221	28660
FJ-02 Spike 25 ng	35228,4	13,24	18,45	9733,7	13,21	38010
FJ-01 Spike 50 ng	93092,7	13,23	45,50	28877	13,232	40323
KJ-01	1885,13	13,26	3,18	635,35	13,199	12866
KJ-02	3084,29	13,23	2,73	375,23	13,188	24999
KJ-03	3166,91	13,24	2,98	1027,8	13,221	23224
NÅS 01 10x	118751	13,25	468,70	36491	13,232	4961,7
NÅS 02 10x	328815	13,28	2212,28	99522	13,253	2909,2
NÅS 03	12927,1	13,31	5,24	4029,2	13,308	51363
NÅV 01A 10x	117443	13,27	725,27	36278	13,264	3170,4
NÅV 01B 10x	101967	13,28	609,49	31967	13,318	3275,8
NÅV 02 A 10x	63649,8	13,3	319,83	20452	13,286	3898,5
NÅV 02 B 10x	9282,87	13,25	318,13	2987,3	13,253	571,6
Br-PFOS L-PFOS STD	78907,9	13,26	24,35	23841	13,275	64241
Br-PFOS L-PFOS STD	78865,8	13,27	25,88	23765	13,286	60384
Br-PFOS L-PFOS STD	79572,4	13,23	24,92	24710	13,221	63291
Br-PFOS L-PFOS STD	75467,9	13,29	24,47	22593	13,275	61144
Br-PFOS L-PFOS STD	77221,3	13,26	24,87	23603	13,232	61546

B

	P1MHpS Results			MPFOS (ISTD) Results	
Name	Area	RT	Calc. Conc.	RT	Resp.
Br-PFOS P1 STD	354245	12,98	64,46	13,329	51610
Br-PFOS P1P55 STD	316254	13,01	40,53	13,34	73278
Br-PFOS P1P55 STD	210426	13,01	24,78	13,351	79710
Br-PFOS P1P55 STD	99686,3	13	9,60	13,351	97366
Br-PFOS P1P55 STD	8493,38	12,98	1,14	13,318	69057
Br-PFOS P1P55 STD	3314,76	12,95	0,45	13,318	67631
FJ-01	325,442	12,83	0,14	13,253	19873
FJ-02	280,531	12,82	0,13	13,221	18717
FJ-03	389,997	12,91	0,09	13,232	35611
FJ-03 Spike 1 ng	3627	12,86	1,18	13,221	28660
FJ-02 Spike 25 ng	83456,6	12,88	20,61	13,21	38010
FJ-01 Spike 50 ng	222014	12,85	51,70	13,232	40323
vask					
blank	13,4067		42,14	13,167	2,9876
KJ-01	88,0728	12,84	0,20	13,199	12710
KJ-02	71,3126	12,86	0,17	13,188	24999
KJ-03	36,5163	12,83	0,15	13,221	23224
NÅS 01 10x	8932	12,88	16,90	13,232	4961,7
NÅS 02 10x	12981,5	12,95	41,90	13,253	2909,2
NÅS 03	372,108	12,96	0,05	13,308	51363
NÅV 01A 10x	10049,6	12,89	29,76	13,264	3170,4
NÅV 01B 10x	8848,34	12,92	25,36	13,318	3275,8
NÅV 02 A 10x	5384,46	12,92	12,96	13,286	3898,5
NÅV 02 B 10x	1267,41	12,86	20,65	13,253	576,22
metodeblank MB	70,693		0,09	13,264	6639,6
Br-PFOS P1P55 STD	269506	12,92	24,69	13,264	102465
Br-PFOS P1P55 STD	266390	12,95	24,49	13,297	102114
Br-PFOS P1P55 STD	263963	12,97	24,98	13,308	99209
Br-PFOS P1P55 STD	262329	12,99	24,44	13,308	100747
Br-PFOS P1P55 STD	265288	12,88	24,96	13,232	99764

C

	P6MHpS Results			MPFOS (ISTD) Results	
Name	RT	Resp.	Calc. Conc.	RT	Resp.
P6 STD 50 ng	12,32	139379,7	50,03	13,373	73050
P6P45 STD 40 ng	12,36	117977,6	40,71	13,351	75997
P6P45 STD 25 ng	12,34	76059,74	24,73	13,373	80655
P6P45 STD 10 ng	12,3	31176,36	10,00	13,308	81728
P6P45 STD 1 ng	12,37	1943,737	0,63	13,373	81153
P6P45 STD 0,5 ng	12,21	1116,092	0,40	13,34	73226
FJ-01	11,98	515,7495	0,68	13,253	19873
FJ-02	12,21	415,3512	0,58	13,221	18717
FJ-03	12,11	873,7573	0,64	13,232	35611
FJ-03 Spike 1 ng	12,08	1758,093	1,61	13,221	28660
FJ-02 Spike 25 ng	12,1	34358,97	23,70	13,21	38010
FJ-01 Spike 50 ng	12,08	105390,5	68,54	13,232	40323
KJ-01	11,91	362,7536	0,74	13,199	12866
KJ-02	12,11	621,6633	0,65	13,188	24999
KJ-03	12,02	605,4618	0,68	13,221	23224
NÅS 01 10x	12,14	12561,62	66,39	13,232	4961,7
NÅS 02 10x	12,16	31834,05	286,94	13,253	2909,2
NÅS 03	12,16	1231,672	0,63	13,308	51363
NÅV 01A 10x	12,18	22294,5	184,40	13,264	3170,4
NÅV 01B 10x	12,19	20238,86	162,01	13,318	3275,8
NÅV 02 A 10x	12,24	10716,26	72,08	13,286	3898,5
NÅV 02 B 10x	12,11	2037,497	92,46	13,253	577,85
metodeblank MB	12,43	21,80005	0,09	13,264	6639,6
Felt blank FB	12,3	4,262649	4,00	13,308	27,93
lagringsblank LB	12,28	5,708427	3,35	13,286	44,641
Br-PFOS P6P45 STD	12,08	93739,95	22,85	13,243	107583
Br-PFOS P6P45 STD	12,17	92602,58	23,45	13,253	103532
Br-PFOS P6P45 STD	12,1	88239,39	22,59	13,264	102412
Br-PFOS P6P45 STD	12,07	89915,64	23,16	13,232	101796
Br-PFOS P6P45 STD	12,16	87138,93	23,31	13,264	98042

D

	P4MHpS Results			MPFOS (ISTD) Results	
Name	RT	Resp.	Calc. Conc.	RT	Resp.
mobilfasekalibrering	9,444	12,8143	13,14	13,08003333	3,8148
mobilfasekalibrering	9,522	7,91714			
mobilfasekalibrering	9,201	13,612			
Vask					
FJ-01	9,92	1367,3	0,49	12,7788	26216
FJ-02	9,6	1180,59	0,51	12,55528333	19945
FJ-03	9,736	2133,04	0,52	12,67188333	35258
FJ-03 Spike 1 ng	9,774	9448,61	1,48	12,66218333	30281
FJ-02 Spike 25 ng	9,211	245613	22,47	12,24431667	42347
FJ-01 Spike 50 ng	9,289	638427	55,93	12,2443	43891
vask					
KJ-01	9,104	1318,75	0,61	12,18601667	15634
KJ-02	8,91	2436,91	0,66	11,90418333	24684
KJ-03	8,744	1845,74	0,57	11,75843333	25071
NÅS 01 10x	9,094	35382,2	20,70	12,25405	6630,8
NÅS 02 10x	9,269	100938	103,37	12,20545	3745,8
NÅS 03	9,541	3549,76	0,53	12,57471667	55909
NÅV 01A 10x	9,483	60461,8	72,53	12,45811667	3201,4
NÅV 01B 10x	9,541	10186,8	10,50	12,44838333	3814,8
NÅV 02 A 10x	9,084	23115,5	19,03	12,14713333	4717,4
NÅV 02 B 10x	9,337	4513,66	29,91	12,51641667	582,77
vask					
metodeblank MB	9,269	62,6556	0,31	12,63303333	8327,7
Felt blank FB	10,45	8,21526	3,30	12,48726667	10,421
lagringsblank LB	8,997	2,12771	1,16	13,44933333	9,2645
vask					
vask					
Co STD 50 ng	10,15	994334	52,71	12,8954	72558
Co STD 40 ng	9,58	801580	38,00	12,565	81303
Co STD 25 ng	9,327	500716	24,38	12,40953333	79489
Co STD 10 ng	9,289	164325	9,77	12,37063333	66250
Co STD 1 ng	9,337	16024,4	1,22	12,33178333	65417
Co STD 0.5 ng	9,259	2316,3	0,41	12,25403333	71315
Co STD 0.1 ng	9,298	2318,24	0,41	12,32203333	68767

E

	P55DMHpS Results			MPFOS (ISTD) Results	
Name	RT	Resp.	Calc. Conc.	RT	Resp.
mobilfasekalibrering	8,054	20,5305	25,66	13,08	3,81
mobilfasekalibrering	8,025	29,8104			
mobilfasekalibrering	7,966	9,58312			
Vask					
FJ-01	7,86	9,39254	0,00	12,78	26216,06
FJ-02	7,908	21,1563	0,01	12,56	19945,34
FJ-03	7,869	10,7694	0,00	12,67	35257,59
FJ-03 Spike 1 ng	7,655	5265,86	0,83	12,66	30281,17
FJ-02 Spike 25 ng	7,549	193992	21,84	12,24	42347,25
FJ-01 Spike 50 ng	7,665	481484	52,31	12,24	43890,56
vask					
KJ-01	7,442	9,22867	0,00	12,19	15634,26
KJ-02	8,637	75,6849	0,01	11,90	24684,10
KJ-03	8,549	53,1055	0,01	11,76	25071,29
NÅS 01 10x	7,539	244,693	0,18	12,25	6630,81
NÅS 02 10x	7,86	185,588	0,24	12,21	3745,77
NÅS 03	7,753	10,0078	0,00	12,57	55908,66
NÅV 01A 10x	7,996	118,917	0,18	12,46	3201,40
NÅV 01B 10x	8,171	144,057	0,18	12,45	3814,80
NÅV 02 A 10x	7,5	1031,61	1,04	12,15	4717,39
NÅV 02 B 10x	8,054	14,0381	0,11	12,52	582,77
vask					
metodeblank MB	7,85	105,439	0,06	12,63	8327,66
Felt blank FB	8,19	6,53501	2,99	12,49	10,42
lagringsblank LB	7,617	9,41695	4,85	13,45	9,26
vask					
vask					
Co STD 50 ng	8,248	833312	54,76	12,90	72558,42
Co STD 40 ng	7,743	650907	38,17	12,57	81303,08
Co STD 25 ng	7,51	385866	23,15	12,41	79489,28
Co STD 10 ng	7,461	131263	9,45	12,37	66249,96
Co STD 1 ng	7,364	11520,5	0,84	12,33	65417,43
Co STD 0.5 ng	7,519	1970,51	0,13	12,25	71314,68
Co STD 0.1 ng	7,655	2064,1	0,14	12,32	68766,89

Appendix H: Worklists for the analytical method

Table 6: Worklist for quantifications from the samples in this study for the isomers that was quantified separately (A) with calibration curves of all isomers and for the coeluting isomers (B).

A

	Sample Name	Sample Position	Method	Data File	Sample Type
1	mobilfasekalibrering		D:\MassHunter\Methods\Mathias\C18 metode utvikling\Br-PFOS metode test brattere gradient 1.m	D:\MassHunter\Data\Mathias (MAB)\Vannprøver FJ og KJ\kalibrering mobilfase.d	Blank
2	Br-PFOS P5 STD	P2-C1	D:\MassHunter\Methods\Mathias\C18 metode utvikling\Br-PFOS metode test brattere gradient 1.m	D:\MassHunter\Data\Mathias (MAB)\Vannprøver FJ og KJ\kalibreringsrekke P5 50ng-r001.d	Calibration
3	Br-PFOS P5 STD	P2-C2	D:\MassHunter\Methods\Mathias\C18 metode utvikling\Br-PFOS metode test brattere gradient 1.m	D:\MassHunter\Data\Mathias (MAB)\Vannprøver FJ og KJ\kalibreringsrekke P5 40ng-r001.d	Calibration
4	Br-PFOS P5 STD	P2-C3	D:\MassHunter\Methods\Mathias\C18 metode utvikling\Br-PFOS metode test brattere gradient 1.m	D:\MassHunter\Data\Mathias (MAB)\Vannprøver FJ og KJ\kalibreringsrekke P5 25ng-r001.d	Calibration
5	Br-PFOS P5 STD	P2-C4	D:\MassHunter\Methods\Mathias\C18 metode utvikling\Br-PFOS metode test brattere gradient 1.m	D:\MassHunter\Data\Mathias (MAB)\Vannprøver FJ og KJ\kalibreringsrekke P5 10ng-r001.d	Calibration
6	Br-PFOS P5 STD	P2-C5	D:\MassHunter\Methods\Mathias\C18 metode utvikling\Br-PFOS metode test brattere gradient 1.m	D:\MassHunter\Data\Mathias (MAB)\Vannprøver FJ og KJ\kalibreringsrekke P5 1ng-r001.d	Calibration
7	Br-PFOS P5 STD	P2-C6	D:\MassHunter\Methods\Mathias\C18 metode utvikling\Br-PFOS metode test brattere gradient 1.m	D:\MassHunter\Data\Mathias (MAB)\Vannprøver FJ og KJ\kalibreringsrekke P5 0,5-r001.d	Calibration
8	Br-PFOS P6 STD	P1-C1	D:\MassHunter\Methods\Mathias\C18 metode utvikling\Br-PFOS metode test brattere gradient 1.m	D:\MassHunter\Data\Mathias (MAB)\Vannprøver FJ og KJ\kalibreringsrekke P6 50ng-r001.d	Calibration
9	Br-PFOS P45 STD	P1-C2	D:\MassHunter\Methods\Mathias\C18 metode utvikling\Br-PFOS metode test brattere gradient 1.m	D:\MassHunter\Data\Mathias (MAB)\Vannprøver FJ og KJ\kalibreringsrekke P45 50ng-r001.d	Calibration
10	Br-PFOS P6P45 STD	P1-C3	D:\MassHunter\Methods\Mathias\C18 metode utvikling\Br-PFOS metode test brattere gradient 1.m	D:\MassHunter\Data\Mathias (MAB)\Vannprøver FJ og KJ\kalibreringsrekke P6P45 40ng-r001.d	Calibration
11	Br-PFOS P6P45 STD	P1-C4	D:\MassHunter\Methods\Mathias\C18 metode utvikling\Br-PFOS metode test brattere gradient 1.m	D:\MassHunter\Data\Mathias (MAB)\Vannprøver FJ og KJ\kalibreringsrekke P6P45 25ng-r001.d	Calibration
12	Br-PFOS P6P45 STD	P1-C5	D:\MassHunter\Methods\Mathias\C18 metode utvikling\Br-PFOS metode test brattere gradient 1.m	D:\MassHunter\Data\Mathias (MAB)\Vannprøver FJ og KJ\kalibreringsrekke P6P45 10ng-r001.d	Calibration
13	Br-PFOS P6P45 STD	P1-C6	D:\MassHunter\Methods\Mathias\C18 metode utvikling\Br-PFOS metode test brattere gradient 1.m	D:\MassHunter\Data\Mathias (MAB)\Vannprøver FJ og KJ\kalibreringsrekke P6P45 1ng-r001.d	Calibration
14	Br-PFOS P6P45 STD	P1-C7	D:\MassHunter\Methods\Mathias\C18 metode utvikling\Br-PFOS metode test brattere gradient 1.m	D:\MassHunter\Data\Mathias (MAB)\Vannprøver FJ og KJ\kalibreringsrekke P6P45 0,5-r001.d	Calibration
15	Br-PFOS P1 STD	P1-D1	D:\MassHunter\Methods\Mathias\C18 metode utvikling\Br-PFOS metode test brattere gradient 1.m	D:\MassHunter\Data\Mathias (MAB)\Vannprøver FJ og KJ\kalibreringsrekke P1 50ng-r001.d	Calibration
16	Br-PFOS P55 STD	P1-D2	D:\MassHunter\Methods\Mathias\C18 metode utvikling\Br-PFOS metode test brattere gradient 1.m	D:\MassHunter\Data\Mathias (MAB)\Vannprøver FJ og KJ\kalibreringsrekke P55 50ng-r001.d	Calibration
17	Br-PFOS P1P55 STD	P1-D3	D:\MassHunter\Methods\Mathias\C18 metode utvikling\Br-PFOS metode test brattere gradient 1.m	D:\MassHunter\Data\Mathias (MAB)\Vannprøver FJ	Calibration

				og KJ\kalibreringsrekke P1P55 40ng-r001.d	
18	Br-PFOS P1P55 STD	P1-D4	D:\MassHunter\Methods\Mathias\C18 metode utvikling\Br-PFOS metode test brattere gradient 1.m	D:\MassHunter\Data\Mathias (MAB)\\Vannprøver FJ og KJ\kalibreringsrekke P1P55 25ng-r001.d	Calibration
19	Br-PFOS P1P55 STD	P1-D5	D:\MassHunter\Methods\Mathias\C18 metode utvikling\Br-PFOS metode test brattere gradient 1.m	D:\MassHunter\Data\Mathias (MAB)\\Vannprøver FJ og KJ\kalibreringsrekke P1P55 10ng-r001.d	Calibration
20	Br-PFOS P1P55 STD	P1-D6	D:\MassHunter\Methods\Mathias\C18 metode utvikling\Br-PFOS metode test brattere gradient 1.m	D:\MassHunter\Data\Mathias (MAB)\\Vannprøver FJ og KJ\kalibreringsrekke P1P55 1ng-r001.d	Calibration
21	Br-PFOS P1P55 STD	P1-D7	D:\MassHunter\Methods\Mathias\C18 metode utvikling\Br-PFOS metode test brattere gradient 1.m	D:\MassHunter\Data\Mathias (MAB)\\Vannprøver FJ og KJ\kalibreringsrekke P1P55 0,5-r001.d	Calibration
22	Br-PFOS L-PFOS STD	P1-E1	D:\MassHunter\Methods\Mathias\C18 metode utvikling\Br-PFOS metode test brattere gradient 1.m	D:\MassHunter\Data\Mathias (MAB)\\Vannprøver FJ og KJ\kalibreringsrekke LPFOS 50ng-r001.d	Calibration
23	Br-PFOS L-PFOS STD	P1-E2	D:\MassHunter\Methods\Mathias\C18 metode utvikling\Br-PFOS metode test brattere gradient 1.m	D:\MassHunter\Data\Mathias (MAB)\\Vannprøver FJ og KJ\kalibreringsrekke LPFOS 40ng-r001.d	Calibration
24	Br-PFOS L-PFOS STD	P1-E3	D:\MassHunter\Methods\Mathias\C18 metode utvikling\Br-PFOS metode test brattere gradient 1.m	D:\MassHunter\Data\Mathias (MAB)\\Vannprøver FJ og KJ\kalibreringsrekke LPFOS 25ng-r001.d	Calibration
25	Br-PFOS L-PFOS STD	P1-E4	D:\MassHunter\Methods\Mathias\C18 metode utvikling\Br-PFOS metode test brattere gradient 1.m	D:\MassHunter\Data\Mathias (MAB)\\Vannprøver FJ og KJ\kalibreringsrekke LPFOS 10ng-r001.d	Calibration
26	Br-PFOS L-PFOS STD	P1-E5	D:\MassHunter\Methods\Mathias\C18 metode utvikling\Br-PFOS metode test brattere gradient 1.m	D:\MassHunter\Data\Mathias (MAB)\\Vannprøver FJ og KJ\kalibreringsrekke LPFOS 1ng-r001.d	Calibration
27	Br-PFOS L-PFOS STD	P1-E6	D:\MassHunter\Methods\Mathias\C18 metode utvikling\Br-PFOS metode test brattere gradient 1.m	D:\MassHunter\Data\Mathias (MAB)\\Vannprøver FJ og KJ\kalibreringsrekke LPFOS 0,5-r001.d	Calibration
28	Br-PFOS P4 STD	P1-F1	D:\MassHunter\Methods\Mathias\C18 metode utvikling\Br-PFOS metode test brattere gradient 1.m	D:\MassHunter\Data\Mathias (MAB)\\Vannprøver FJ og KJ\kalibreringsrekke P4 50ng-r001.d	Calibration
29	Br-PFOS P4 STD	P1-F2	D:\MassHunter\Methods\Mathias\C18 metode utvikling\Br-PFOS metode test brattere gradient 1.m	D:\MassHunter\Data\Mathias (MAB)\\Vannprøver FJ og KJ\kalibreringsrekke P4 40ng-r001.d	Calibration
30	Br-PFOS P4 STD	P1-F3	D:\MassHunter\Methods\Mathias\C18 metode utvikling\Br-PFOS metode test brattere gradient 1.m	D:\MassHunter\Data\Mathias (MAB)\\Vannprøver FJ og KJ\kalibreringsrekke P4 25ng-r001.d	Calibration
31	Br-PFOS P4 STD	P1-F4	D:\MassHunter\Methods\Mathias\C18 metode utvikling\Br-PFOS metode test brattere gradient 1.m	D:\MassHunter\Data\Mathias (MAB)\\Vannprøver FJ og KJ\kalibreringsrekke P4 10ng-r001.d	Calibration
32	Br-PFOS P4 STD	P1-F5	D:\MassHunter\Methods\Mathias\C18 metode utvikling\Br-PFOS metode test brattere gradient 1.m	D:\MassHunter\Data\Mathias (MAB)\\Vannprøver FJ og KJ\kalibreringsrekke P4 1ng-r001.d	Calibration
33	Br-PFOS P4 STD	P1-F6	D:\MassHunter\Methods\Mathias\C18 metode utvikling\Br-PFOS metode test brattere gradient 1.m	D:\MassHunter\Data\Mathias (MAB)\\Vannprøver FJ og KJ\kalibreringsrekke P4 0,5-r001.d	Calibration
34	Br-PFOS P3 STD	P1-B1	D:\MassHunter\Methods\Mathias\C18 metode utvikling\Br-PFOS metode test brattere gradient 1.m	D:\MassHunter\Data\Mathias (MAB)\\Vannprøver FJ og KJ\kalibreringsrekke P3 50ng-r001.d	Calibration
35	Br-PFOS P3 STD	P1-B2	D:\MassHunter\Methods\Mathias\C18 metode utvikling\Br-PFOS metode test brattere gradient 1.m	D:\MassHunter\Data\Mathias (MAB)\\Vannprøver FJ og KJ\kalibreringsrekke P3 40ng-r001.d	Calibration
36	Br-PFOS P3 STD	P1-B3	D:\MassHunter\Methods\Mathias\C18 metode utvikling\Br-PFOS metode test brattere gradient 1.m	D:\MassHunter\Data\Mathias (MAB)\\Vannprøver FJ og KJ\kalibreringsrekke P3 25ng-r001.d	Calibration
37	Br-PFOS P3 STD	P1-B4	D:\MassHunter\Methods\Mathias\C18 metode utvikling\Br-PFOS metode test brattere gradient 1.m	D:\MassHunter\Data\Mathias (MAB)\\Vannprøver FJ og KJ\kalibreringsrekke P3 10ng-r001.d	Calibration
38	Br-PFOS P3 STD	P1-B5	D:\MassHunter\Methods\Mathias\C18 metode utvikling\Br-PFOS metode test brattere gradient 1.m	D:\MassHunter\Data\Mathias (MAB)\\Vannprøver FJ	Calibration

				og KJ\kalibreringsrekke P3 1ng-r001.d	
39	Br-PFOS P3 STD	P1-B6	D:\MassHunter\Methods\Mathias\C18 metode utvikling\Br-PFOS metode test brattere gradient 1.m	D:\MassHunter\Data\Mathias (MAB)\Vannprøver FJ og KJ\kalibreringsrekke P3 0,5-r001.d	Calibration
40	Vask		D:\MassHunter\Methods\Mathias\ACE-C18 PFP metodevask.m	D:\MassHunter\Data\Mathias (MAB)\Vannprøver FJ og KJ\Vask.d	Sample
41	blank		D:\MassHunter\Methods\Mathias\C18 metode utvikling\Br-PFOS metode test brattere gradient 1.m	D:\MassHunter\Data\Mathias (MAB)\Vannprøver FJ og KJ\Blank.d	Blank
42	FJ-01	P2-D1	D:\MassHunter\Methods\Mathias\C18 metode utvikling\Br-PFOS metode test brattere gradient 1.m	D:\MassHunter\Data\Mathias (MAB)\Vannprøver FJ og KJ\FJ-01-r001.d	Sample
43	FJ-02	P2-D2	D:\MassHunter\Methods\Mathias\C18 metode utvikling\Br-PFOS metode test brattere gradient 1.m	D:\MassHunter\Data\Mathias (MAB)\Vannprøver FJ og KJ\FJ-02-r001.d	Sample
44	FJ-03	P2-D3	D:\MassHunter\Methods\Mathias\C18 metode utvikling\Br-PFOS metode test brattere gradient 1.m	D:\MassHunter\Data\Mathias (MAB)\Vannprøver FJ og KJ\FJ-03-r001.d	Sample
45	FJ-03 Spike 1 ng	P2-D6	D:\MassHunter\Methods\Mathias\C18 metode utvikling\Br-PFOS metode test brattere gradient 1.m	D:\MassHunter\Data\Mathias (MAB)\Vannprøver FJ og KJ\FJ-01 spike 1-r001.d	Sample
46	FJ-02 Spike 25 ng	P2-D5	D:\MassHunter\Methods\Mathias\C18 metode utvikling\Br-PFOS metode test brattere gradient 1.m	D:\MassHunter\Data\Mathias (MAB)\Vannprøver FJ og KJ\FJ-01 spike 25-r001.d	Sample
47	FJ-01 Spike 50 ng	P2-D4	D:\MassHunter\Methods\Mathias\C18 metode utvikling\Br-PFOS metode test brattere gradient 1.m	D:\MassHunter\Data\Mathias (MAB)\Vannprøver FJ og KJ\FJ-01 spike 50-r001.d	Sample
48	vask		D:\MassHunter\Methods\Mathias\ACE-C18 PFP metodevask.m	D:\MassHunter\Data\Mathias (MAB)\Vannprøver FJ og KJ\Vask 2.d	Sample
49	blank		D:\MassHunter\Methods\Mathias\C18 metode utvikling\Br-PFOS metode test brattere gradient 1.m	D:\MassHunter\Data\Mathias (MAB)\Vannprøver FJ og KJ\Blank 2.d	Blank
50	KJ-01	P2-D7	D:\MassHunter\Methods\Mathias\C18 metode utvikling\Br-PFOS metode test brattere gradient 1.m	D:\MassHunter\Data\Mathias (MAB)\Vannprøver FJ og KJ\KJ-01.d	Sample
51	KJ-02	P2-D8	D:\MassHunter\Methods\Mathias\C18 metode utvikling\Br-PFOS metode test brattere gradient 1.m	D:\MassHunter\Data\Mathias (MAB)\Vannprøver FJ og KJ\KJ-02.d	Sample
52	KJ-03	P2-D9	D:\MassHunter\Methods\Mathias\C18 metode utvikling\Br-PFOS metode test brattere gradient 1.m	D:\MassHunter\Data\Mathias (MAB)\Vannprøver FJ og KJ\KJ-03.d	Sample
53	NÅS 01 10x	P2-A1	D:\MassHunter\Methods\Mathias\C18 metode utvikling\Br-PFOS metode test brattere gradient 1.m	D:\MassHunter\Data\Mathias (MAB)\Vannprøver FJ og KJ\NÅS 01.d	Sample
54	NÅS 02 10x	P2-A2	D:\MassHunter\Methods\Mathias\C18 metode utvikling\Br-PFOS metode test brattere gradient 1.m	D:\MassHunter\Data\Mathias (MAB)\Vannprøver FJ og KJ\NÅS 02.d	Sample
55	NÅS 03	P2-A3	D:\MassHunter\Methods\Mathias\C18 metode utvikling\Br-PFOS metode test brattere gradient 1.m	D:\MassHunter\Data\Mathias (MAB)\Vannprøver FJ og KJ\NÅS 03.d	Sample
56	NÅV 01A 10x	P2-B1	D:\MassHunter\Methods\Mathias\C18 metode utvikling\Br-PFOS metode test brattere gradient 1.m	D:\MassHunter\Data\Mathias (MAB)\Vannprøver FJ og KJ\NÅV 01A.d	Sample
57	NÅV 01B 10x	P2-B2	D:\MassHunter\Methods\Mathias\C18 metode utvikling\Br-PFOS metode test brattere gradient 1.m	D:\MassHunter\Data\Mathias (MAB)\Vannprøver FJ og KJ\NÅV 01B.d	Sample
58	NÅV 02 A 10x	P2-B3	D:\MassHunter\Methods\Mathias\C18 metode utvikling\Br-PFOS metode test brattere gradient 1.m	D:\MassHunter\Data\Mathias (MAB)\Vannprøver FJ og KJ\NÅV 02A.d	Sample
59	NÅV 02 B 10x	P2-B4	D:\MassHunter\Methods\Mathias\C18 metode utvikling\Br-PFOS metode test brattere gradient 1.m	D:\MassHunter\Data\Mathias (MAB)\Vannprøver FJ og KJ\NÅV 02B.d	Sample
60	vask		D:\MassHunter\Methods\Mathias\ACE-C18 PFP metodevask.m	D:\MassHunter\Data\Mathias (MAB)\Vannprøver FJ og KJ\Vask 3.d	Sample
61	blank		D:\MassHunter\Methods\Mathias\C18 metode utvikling\Br-PFOS metode test brattere gradient 1.m	D:\MassHunter\Data\Mathias (MAB)\Vannprøver FJ og KJ\Blank 3.d	Blank
62	metodeblank MB	P2-E1	D:\MassHunter\Methods\Mathias\C18 metode utvikling\Br-PFOS metode test brattere gradient 1.m	D:\MassHunter\Data\Mathias (MAB)\Vannprøver FJ og KJ\metodeblank.d	Blank
63	Felt blank FB	P2-E2	D:\MassHunter\Methods\Mathias\C18 metode utvikling\Br-PFOS metode test brattere gradient 1.m	D:\MassHunter\Data\Mathias (MAB)\Vannprøver FJ og KJ\feltblank.d	Blank
64	lagringsblank LB	P2-E3	D:\MassHunter\Methods\Mathias\C18 metode utvikling\Br-PFOS metode test brattere gradient 1.m	D:\MassHunter\Data\Mathias (MAB)\Vannprøver FJ og KJ\lagringsblank.d	Blank

65	vask		D:\MassHunter\Methods\Mathias\ACE-C18 PFP metodevask.m	D:\MassHunter\Data\Mathias (MAB)\Vannprøver FJ og KJ\Vask 4 siste 1.d	Sample
66	vask		D:\MassHunter\Methods\Mathias\ACE-C18 PFP metodevask.m	D:\MassHunter\Data\Mathias (MAB)\Vannprøver FJ og KJ\Vask 4 siste 2.d	Sample

B

1	mobilfasekalibrering		D:\MassHunter\Methods\Mathias\C18 metode utvikling\Br-PFOS metode test brattere gradient 1.m	D:\MassHunter\Data\Mathias (MAB)\Vannprøver FJ og KJ\kalibrering mobilfase 1.d	Sample
2	mobilfasekalibrering		D:\MassHunter\Methods\Mathias\C18 metode utvikling\Br-PFOS metode test brattere gradient 1.m	D:\MassHunter\Data\Mathias (MAB)\Vannprøver FJ og KJ\kalibrering mobilfase 2.d	Sample
3	mobilfasekalibrering		D:\MassHunter\Methods\Mathias\C18 metode utvikling\Br-PFOS metode test brattere gradient 1.m	D:\MassHunter\Data\Mathias (MAB)\Vannprøver FJ og KJ\kalibrering test 2.d	Blank
4	Co STD 50 ng	P2-C1	D:\MassHunter\Methods\Mathias\C18 metode utvikling\Br-PFOS metode test brattere gradient 1.m	D:\MassHunter\Data\Mathias (MAB)\Vannprøver FJ og KJ\kalibreringsrekke CoSTD 50ng-r001 test 2.d	Calibration
5	Co STD 40 ng	P2-C2	D:\MassHunter\Methods\Mathias\C18 metode utvikling\Br-PFOS metode test brattere gradient 1.m	D:\MassHunter\Data\Mathias (MAB)\Vannprøver FJ og KJ\kalibreringsrekke CoSTD 40ng test 2.d	Calibration
6	Co STD 25 ng	P2-C3	D:\MassHunter\Methods\Mathias\C18 metode utvikling\Br-PFOS metode test brattere gradient 1.m	D:\MassHunter\Data\Mathias (MAB)\Vannprøver FJ og KJ\kalibreringsrekke CoSTD 25ng test 2.d	Calibration
7	Co STD 10 ng	P2-C4	D:\MassHunter\Methods\Mathias\C18 metode utvikling\Br-PFOS metode test brattere gradient 1.m	D:\MassHunter\Data\Mathias (MAB)\Vannprøver FJ og KJ\kalibreringsrekke CoSTD 10ng test 2.d	Calibration
8	Co STD 1 ng	P2-C5	D:\MassHunter\Methods\Mathias\C18 metode utvikling\Br-PFOS metode test brattere gradient 1.m	D:\MassHunter\Data\Mathias (MAB)\Vannprøver FJ og KJ\kalibreringsrekke CoSTD 1ng test 2.d	Calibration
9	Co STD 0.5 ng	P2-C6	D:\MassHunter\Methods\Mathias\C18 metode utvikling\Br-PFOS metode test brattere gradient 1.m	D:\MassHunter\Data\Mathias (MAB)\Vannprøver FJ og KJ\kalibreringsrekke CoSTD 0.5ng test 2.d	Calibration
10	Co STD 0.1 ng	P2-C6	D:\MassHunter\Methods\Mathias\C18 metode utvikling\Br-PFOS metode test brattere gradient 1.m	D:\MassHunter\Data\Mathias (MAB)\Vannprøver FJ og KJ\kalibreringsrekke CoSTD 0.1ng test 2.d	Calibration
11	Vask		D:\MassHunter\Methods\Mathias\ACE-C18 PFP metodevask.m	D:\MassHunter\Data\Mathias (MAB)\Vannprøver FJ og KJ\Vask.d	Sample
12	blank		D:\MassHunter\Methods\Mathias\C18 metode utvikling\Br-PFOS metode test brattere gradient 1.m	D:\MassHunter\Data\Mathias (MAB)\Vannprøver FJ og KJ\Blank.d	Blank
13	FJ-01	P2-D1	D:\MassHunter\Methods\Mathias\C18 metode utvikling\Br-PFOS metode test brattere gradient 1.m	D:\MassHunter\Data\Mathias (MAB)\Vannprøver FJ og KJ\FJ-01-r001.d	Sample
14	FJ-02	P2-D2	D:\MassHunter\Methods\Mathias\C18 metode utvikling\Br-PFOS metode test brattere gradient 1.m	D:\MassHunter\Data\Mathias (MAB)\Vannprøver FJ og KJ\FJ-02-r001.d	Sample
15	FJ-03	P2-D3	D:\MassHunter\Methods\Mathias\C18 metode utvikling\Br-PFOS metode test brattere gradient 1.m	D:\MassHunter\Data\Mathias (MAB)\Vannprøver FJ og KJ\FJ-03-r001.d	Sample
16	FJ-03 Spike 1 ng	P2-D6	D:\MassHunter\Methods\Mathias\C18 metode utvikling\Br-PFOS metode test brattere gradient 1.m	D:\MassHunter\Data\Mathias (MAB)\Vannprøver FJ og KJ\FJ-01 spike 1-r001.d	Sample
17	FJ-02 Spike 25 ng	P2-D5	D:\MassHunter\Methods\Mathias\C18 metode utvikling\Br-PFOS metode test brattere gradient 1.m	D:\MassHunter\Data\Mathias (MAB)\Vannprøver FJ og KJ\FJ-01 spike 25-r001.d	Sample
18	FJ-01 Spike 50 ng	P2-D4	D:\MassHunter\Methods\Mathias\C18 metode utvikling\Br-PFOS metode test brattere gradient 1.m	D:\MassHunter\Data\Mathias (MAB)\Vannprøver FJ og KJ\FJ-01 spike 50-r001.d	Sample
19	vask		D:\MassHunter\Methods\Mathias\ACE-C18 PFP metodevask.m	D:\MassHunter\Data\Mathias (MAB)\Vannprøver FJ og KJ\Vask 2.d	Sample
20	blank		D:\MassHunter\Methods\Mathias\C18 metode utvikling\Br-PFOS metode test brattere gradient 1.m	D:\MassHunter\Data\Mathias (MAB)\Vannprøver FJ og KJ\Blank 2.d	Blank
21	KJ-01	P2-D7	D:\MassHunter\Methods\Mathias\C18 metode utvikling\Br-PFOS metode test brattere gradient 1.m	D:\MassHunter\Data\Mathias (MAB)\Vannprøver FJ og KJ\KJ-01.d	Sample

22	KJ-02	P2-D8	D:\MassHunter\Methods\Mathias\C18 metode utvikling\Br-PFOS metode test brattere gradient 1.m	D:\MassHunter\Data\Mathias (MAB)\Vannprøver FJ og KJ\KJ-02.d	Sample
23	KJ-03	P2-D9	D:\MassHunter\Methods\Mathias\C18 metode utvikling\Br-PFOS metode test brattere gradient 1.m	D:\MassHunter\Data\Mathias (MAB)\Vannprøver FJ og KJ\KJ-03.d	Sample
24	NÅS 01 10x	P2-A1	D:\MassHunter\Methods\Mathias\C18 metode utvikling\Br-PFOS metode test brattere gradient 1.m	D:\MassHunter\Data\Mathias (MAB)\Vannprøver FJ og KJ\NÅS 01.d	Sample
25	NÅS 02 10x	P2-A2	D:\MassHunter\Methods\Mathias\C18 metode utvikling\Br-PFOS metode test brattere gradient 1.m	D:\MassHunter\Data\Mathias (MAB)\Vannprøver FJ og KJ\NÅS 02.d	Sample
26	NÅS 03	P2-A3	D:\MassHunter\Methods\Mathias\C18 metode utvikling\Br-PFOS metode test brattere gradient 1.m	D:\MassHunter\Data\Mathias (MAB)\Vannprøver FJ og KJ\NÅS 03.d	Sample
27	NÅV 01A 10x	P2-B1	D:\MassHunter\Methods\Mathias\C18 metode utvikling\Br-PFOS metode test brattere gradient 1.m	D:\MassHunter\Data\Mathias (MAB)\Vannprøver FJ og KJ\NÅV 01A.d	Sample
28	NÅV 01B 10x	P2-B2	D:\MassHunter\Methods\Mathias\C18 metode utvikling\Br-PFOS metode test brattere gradient 1.m	D:\MassHunter\Data\Mathias (MAB)\Vannprøver FJ og KJ\NÅV 01B.d	Sample
29	NÅV 02 A 10x	P2-B3	D:\MassHunter\Methods\Mathias\C18 metode utvikling\Br-PFOS metode test brattere gradient 1.m	D:\MassHunter\Data\Mathias (MAB)\Vannprøver FJ og KJ\NÅV 02A.d	Sample
30	NÅV 02 B 10x	P2-B4	D:\MassHunter\Methods\Mathias\C18 metode utvikling\Br-PFOS metode test brattere gradient 1.m	D:\MassHunter\Data\Mathias (MAB)\Vannprøver FJ og KJ\NÅV 02B.d	Sample
31	vask		D:\MassHunter\Methods\Mathias\ACE-C18 PFP metodevask.m	D:\MassHunter\Data\Mathias (MAB)\Vannprøver FJ og KJ\Vask 3.d	Sample
32	blank		D:\MassHunter\Methods\Mathias\C18 metode utvikling\Br-PFOS metode test brattere gradient 1.m	D:\MassHunter\Data\Mathias (MAB)\Vannprøver FJ og KJ\Blank 3.d	Blank
33	metodeblank MB	P2-E1	D:\MassHunter\Methods\Mathias\C18 metode utvikling\Br-PFOS metode test brattere gradient 1.m	D:\MassHunter\Data\Mathias (MAB)\Vannprøver FJ og KJ\metodeblank.d	Blank
34	Felt blank FB	P2-E2	D:\MassHunter\Methods\Mathias\C18 metode utvikling\Br-PFOS metode test brattere gradient 1.m	D:\MassHunter\Data\Mathias (MAB)\Vannprøver FJ og KJ\feltblank.d	Blank
35	lagringsblank LB	P2-E3	D:\MassHunter\Methods\Mathias\C18 metode utvikling\Br-PFOS metode test brattere gradient 1.m	D:\MassHunter\Data\Mathias (MAB)\Vannprøver FJ og KJ\lagringsblank.d	Blank
36	vask		D:\MassHunter\Methods\Mathias\ACE-C18 PFP metodevask.m	D:\MassHunter\Data\Mathias (MAB)\Vannprøver FJ og KJ\Vask 4 siste 1.d	Sample
37	vask		D:\MassHunter\Methods\Mathias\ACE-C18 PFP metodevask.m	D:\MassHunter\Data\Mathias (MAB)\Vannprøver FJ og KJ\Vask 4 test 2.d	Sample

Appendix I: pictures of the studysites

Figure I-1: Picture of the sampling location in Sogna

Figure 5: picture of the samling location in Fjellhamardammen environmental park.

Norges miljø- og biovitenskapelige universitet
Noregs miljø- og biovitskapelege universitet
Norwegian University of Life Sciences

Postboks 5003
NO-1432 Ås
Norway